

# LEGENDRIAN HOPF LINKS

HANSJÖRG GEIGES AND SINEM ONARAN

ABSTRACT. We completely classify Legendrian realisations of the Hopf link, up to coarse equivalence, in the 3-sphere with any contact structure.

## 1. INTRODUCTION

When we speak of a *Hopf link* in this paper, we shall always mean an ordered link  $K_0 \sqcup K_1$  in the 3-sphere  $S^3$ , made up of oriented unknots forming a *positive* Hopf link, that is,  $K_1$  is isotopic in  $S^3 \setminus K_0$  to a positive meridian of  $K_0$ . Two Legendrian realisations  $L_0 \sqcup L_1$  and  $L'_0 \sqcup L'_1$  of this Hopf link in some contact structure  $\xi$  on  $S^3$  are called *coarsely equivalent* if there is a contactomorphism of  $(S^3, \xi)$  that sends  $L_0 \sqcup L_1$  to  $L'_0 \sqcup L'_1$  as an ordered, oriented link.

The main result of this paper is the classification, up to coarse equivalence, of all Legendrian realisations of the Hopf link in  $S^3$  with any contact structure.

For a brief introduction to the theory of Legendrian knots, i.e. knots tangent to a given contact structure, see [15, Chapter 3] or the beautiful survey by Etnyre [11]. The latter discusses the classification of Legendrian knots and covers a wide range of applications of Legendrian knot theory not only to contact geometry (e.g. surgery along Legendrian knots, invariants of contact structures), but also to general topology (e.g. plane curves, knot concordance, topological knot invariants).

Very little is known about the classification of Legendrian links (with more than one component). When Etnyre wrote his survey on Legendrian and transverse knots in 2005, the results about Legendrian links could be summarised on two pages. Since then, only a small number of classification statements on Legendrian links in the standard tight contact structure  $\xi_{\text{st}}$  on  $S^3$  or in other tight contact 3-manifolds have been added to the literature, e.g. [3, 4]. The present paper goes considerably beyond those results, both concerning the range of Legendrian realisations covered by the classification and the variety of methods used in the proof. Our main theorem is the first complete Legendrian classification of a topological link type that includes Legendrian realisations in overtwisted contact structures.

Legendrian knots in overtwisted contact structures fall into two classes, loose and exceptional. The latter can be divided into two subclasses.

**Definition 1.1.** A Legendrian knot  $L$  in an overtwisted contact 3-manifold  $(M, \xi)$  is called *exceptional* if its complement  $(M \setminus L, \xi|_{M \setminus L})$  is tight; the knot is called *loose* if the contact structure is still overtwisted when restricted to the knot complement.

An exceptional Legendrian knot is called *strongly exceptional* if the knot complement has zero Giroux torsion.

---

2010 *Mathematics Subject Classification.* 57M25; 53D35, 57M27, 57R17.

H. G. is partially supported by the SFB/TRR 191 ‘Symplectic Structures in Geometry, Algebra and Dynamics’, funded by the DFG; S. O. is partially supported by a Turkish Academy of Sciences TÜBA–GEBIP.

The notion of *Giroux torsion* and the related concept of *twisting* will be explained below. Previous classification results for exceptional Legendrian knots such as [18] confined attention to *strongly* exceptional realisations. One of the reasons for this restriction is that classification results for tight contact structures on the relevant knot complement typically tend to require, as in [7], that the Giroux torsion be zero. One of the significant features of our classification of Legendrian Hopf links, by contrast, is the fact that it includes Legendrian realisations where the link complement may contain torsion without being overtwisted.

Here is our main result. As mentioned before,  $\xi_{\text{st}}$  denotes the standard tight contact structure on  $S^3$ . Besides this standard structure, there is a countable family of overtwisted contact structures  $\{\xi_d: d \in \mathbb{Z} + \frac{1}{2}\}$ , as we shall recall below. For the definition of the classical invariants  $\mathbf{tb}$  (Thurston–Bennequin invariant) and  $\mathbf{rot}$  (rotation number) of Legendrian knots, as well as other fundamentals of contact topology, the reader may refer to [15]. Our natural numbers  $\mathbb{N}$  are the positive integers;  $\mathbb{N}_0$  includes zero.

**Theorem 1.2.** *Up to coarse equivalence, the Legendrian realisations of the Hopf link are as follows. In all cases, the classical invariants determine the Legendrian realisation.*

- (a) *In  $(S^3, \xi_{\text{st}})$  there is a unique realisation for any combination of classical invariants  $(\mathbf{tb}, \mathbf{rot}) = (\mathbf{t}_i, \mathbf{r}_i)$ ,  $i = 0, 1$ , in the range  $\mathbf{t}_0, \mathbf{t}_1 < 0$  and*

$$\mathbf{r}_i \in \{\mathbf{t}_i + 1, \mathbf{t}_i + 3, \dots, -\mathbf{t}_i - 3, -\mathbf{t}_i - 1\}.$$

*For fixed values of  $\mathbf{t}_0, \mathbf{t}_1 < 0$  this gives a total of  $\mathbf{t}_0 \mathbf{t}_1$  realisations.*

- (b) *For  $\mathbf{t}_0 < 0$  and  $\mathbf{t}_1 > 0$  the strongly exceptional realisations are as follows.*  
 (b1) *In  $(S^3, \xi_{1/2})$  there are realisations  $L_0 \sqcup L_1$  made up of an exceptional Legendrian unknot  $L_1$  with invariants  $(\mathbf{t}_1, \mathbf{r}_1) = (n + 2, \pm(n + 1))$ , where  $n \in \mathbb{N}_0$ , and a loose Legendrian unknot  $L_0$  whose Thurston–Bennequin invariant  $\mathbf{t}_0$  can be any negative number, and  $\mathbf{r}_0$  lies in the range*

$$\{\mathbf{t}_0, \mathbf{t}_0 + 2, \dots, \mathbf{t}_0 - 2, -\mathbf{t}_0\}.$$

*For a given  $\mathbf{t}_0 < 0$ , this gives us  $2|\mathbf{t}_0 - 1|$  realisations.*

- (b2) *In  $(S^3, \xi_{1/2})$  there are realisations  $L_0 \sqcup L_1$  consisting of the exceptional Legendrian unknot  $L_1$  with invariants  $(\mathbf{t}_1, \mathbf{r}_1) = (1, 0)$  and a loose Legendrian unknot  $L_0$ , where  $\mathbf{t}_0$  can be any negative number, and  $\mathbf{r}_0$  lies in the range*

$$\{\mathbf{t}_0 - 1, \mathbf{t}_0 + 1, \dots, \mathbf{t}_0 - 1, -\mathbf{t}_0 + 1\}.$$

*For a given  $\mathbf{t}_0 < 0$ , these are  $|\mathbf{t}_0 - 2|$  realisations.*

- (c) *For  $\mathbf{t}_0, \mathbf{t}_1 > 0$  the strongly exceptional realisations are as follows.*  
 (c1) *There is a unique realisation in  $(S^3, \xi_{1/2})$  with  $(\mathbf{t}_i, \mathbf{r}_i) = (1, 0)$ ,  $i = 0, 1$ . Both  $L_0$  and  $L_1$  are exceptional.*  
 (c2) *There is a pair of realisations with  $(\mathbf{t}_0, \mathbf{r}_0) = (2, \pm 3)$  and  $(\mathbf{t}_1, \mathbf{r}_1) = (1, \pm 2)$  in  $(S^3, \xi_{-1/2})$ . There are three realisations with  $\mathbf{t}_0 = 3$  and  $\mathbf{t}_1 = 1$ . Two of them with  $(\mathbf{t}_0, \mathbf{r}_0) = (3, \pm 4)$  and  $(\mathbf{t}_1, \mathbf{r}_1) = (1, \pm 2)$  live in  $(S^3, \xi_{-1/2})$ ; the third one with  $(\mathbf{t}_0, \mathbf{r}_0) = (3, 0)$  and  $(\mathbf{t}_1, \mathbf{r}_1) = (1, 0)$  can be found in  $(S^3, \xi_{3/2})$ .*

There are four realisations with  $\mathfrak{t}_0 = \mathfrak{t}_1 = 2$ : two with  $\mathfrak{r}_1 = \mathfrak{r}_2 = \pm 3$  in  $(S^3, \xi_{-1/2})$ , two with  $\mathfrak{r}_0 = \mathfrak{r}_1 = \pm 1$  in  $(S^3, \xi_{3/2})$ .

In all cases, the individual link components are loose.

- (c3) For any  $\mathfrak{t}_0 \geq 4$  and  $\mathfrak{t}_1 = 1$  there are four links realising these values of the Thurston–Bennequin invariants. For  $\mathfrak{t}_0 \geq 3$  and  $\mathfrak{t}_1 = 2$  there are six realisations. The remaining invariants are listed in Table 2 in Section 9. The link components are loose.
- (c4) For each choice of  $\mathfrak{t}_0, \mathfrak{t}_1 \geq 3$  there are eight realisations. In all cases both link components loose. The invariants are listed in Table 2.
- (d) For  $\mathfrak{t}_0 = 0$ , there are two exceptional realisations with  $\mathfrak{t}_1 = m$  for each  $m \in \mathbb{Z}$ . The rotation numbers are  $\mathfrak{r}_0 = \pm 1$  and  $\mathfrak{r}_1 = \pm(m - 1)$ . The unknot  $L_0$  is always loose;  $L_1$  is loose for  $m \leq 0$ , exceptional for  $m \geq 1$ .
- (e) For each choice of integers  $(\mathfrak{t}_0, \mathfrak{t}_1) \neq (\pm 1, \pm 1)$  and natural number  $p$  there is exactly a pair of exceptional Legendrian Hopf links  $L_0 \sqcup L_1$ , distinguished by the rotation numbers, with  $\mathfrak{tb}(L_i) = \mathfrak{t}_i$  and with  $\pi$ -twisting in the link complement equal to  $p$ . For  $\mathfrak{t}_0 = \mathfrak{t}_1 = \pm 1$ , there is a unique realisation. The ambient contact structure is  $\xi_{1/2}$  or  $\xi_{-1/2}$ .
- (f) For any choice of  $\mathfrak{t}_0, \mathfrak{r}_0, \mathfrak{t}_1, \mathfrak{r}_1 \in \mathbb{Z}$  with  $\mathfrak{t}_i + \mathfrak{r}_i$  odd, and for any  $d \in \mathbb{Z} + \frac{1}{2}$ , there is a unique loose Hopf link  $L_0 \sqcup L_1$  in  $(S^3, \xi_d)$  with invariants  $\mathfrak{tb}(L_i) = \mathfrak{t}_i$  and  $\mathfrak{rot}(L_i) = \mathfrak{r}_i$ .

Explicit realisations will be exhibited below. Those examples will give us a complete list of the classical invariants that can be realised. Observe that exceptional realisations of the Hopf link exist only in the three overtwisted structures  $\xi_{\pm 1/2}$  and  $\xi_{3/2}$ .

For easier navigation, here is a guide to the paper, indicating where each part of Theorem 1.2 will be proved. Part (a) about realisations in the tight contact structure, which was proved earlier in [3], will be discussed in Section 4.

The classification of strongly exceptional realisations, parts (b) to (d), is achieved in Section 5, and this takes up the largest part of the paper. In Section 3 we determine the number of tight contact structures on the link complement as a function of the values  $\mathfrak{t}_0, \mathfrak{t}_1$  of the Thurston–Bennequin invariants, using results of Giroux [21] and Honda [24]. This gives an upper bound on the number of Legendrian realisations. We show that this bound is attained in all cases by exhibiting explicit realisations in contact surgery diagrams. This strategy was developed in [17] for the classification of Legendrian rational unknots in lens spaces.

The classification of the Hopf links with twisting in the complement, part (e), will be given in Section 7.4, based on the discussion in the preceding parts of Section 7. The necessary preparations to describe explicit realisations in this case are contained in Section 6, where we construct a couple of overtwisted contact structures on  $S^3$  as contact cuts in the sense of Lerman [26]. We recover some results of Dymara [8] about exceptional realisations of the unknot in this model of  $S^3$ , with considerably simplified arguments.

Statement (f) about the classification of loose Legendrian Hopf links will be proved in Section 8.

## 2. CONTACT STRUCTURES ON $S^3$

Throughout we are dealing with *(co-)oriented* and *positive* contact structures on the 3-sphere  $S^3$ , that is, tangent 2-plane fields  $\xi$  that are described as  $\xi = \ker \alpha$  with

some globally defined 1-form  $\alpha$  satisfying  $\alpha \wedge d\alpha > 0$  with respect to the standard orientation of  $S^3 \subset \mathbb{C}^2$ .

The standard contact structure

$$(1) \quad \xi_{\text{st}} = \ker(x_1 dy_1 - y_1 dx_1 + x_2 dy_2 - y_2 dx_2)$$

on  $S^3$  is the unique tight contact structure, up to isotopy, on the 3-sphere. Furthermore, there is a countable family of overtwisted contact structures. Their classification up to isotopy coincides with their homotopy classification as tangent 2-plane fields.

There are two invariants that equally detect the homotopy class of an oriented tangent 2-plane field  $\xi$  on  $S^3$ . The first one is the Hopf invariant  $h$ . The definition of this invariant presupposes that we fix a trivialisation  $TS^3 \cong S^3 \times \mathbb{R}^3$  of the tangent bundle of  $S^3$ . The Gauß map of  $\xi$  may then be regarded as a map  $S^3 \rightarrow S^2$ , which has a well-defined Hopf invariant  $h \in \mathbb{Z}$ .

Alternatively, one may use the  $d_3$ -invariant introduced by Gompf [22], cf. [5, 23]. This can be computed from any compact almost complex 4-manifold  $(X, J)$  with boundary  $\partial X = S^3$  such that the complex line  $TS^3 \cap J(TS^3)$  in the tangent bundle  $TS^3$  coincides with the oriented plane field  $\xi$ . According to [22, Thm. 4.16], the  $d_3$ -invariant is computed from this data as

$$(2) \quad d_3(\xi) = \frac{1}{4}(c_1^2(X, J) - 3\sigma(X) - 2\chi(X)),$$

where  $c_1$  denotes the first Chern class,  $\sigma$  the signature, and  $\chi$  the Euler characteristic of  $(X, J)$ . Such an almost complex filling  $(X, J)$  of  $(S^3, \xi)$  can always be found, and  $d_3(\xi)$  is independent of the choice of filling. The  $d_3$ -invariant can be defined more generally for any oriented tangent 2-plane field on any closed, oriented 3-manifold, provided the Euler class of  $\xi$  is torsion. Notice that the definition of  $d_3(\xi)$  does not involve a choice of trivialisation of the tangent bundle of the 3-manifold in question.

For  $S^3$  the  $d_3$ -invariant takes values in  $\mathbb{Z} + \frac{1}{2}$ , see [5, Remark 2.6].

**Remark 2.1.** Observe that the Hopf invariant  $h(\xi)$  does not depend on the choice of (co-)orientation of  $\xi$ , since composition with the antipodal map of  $S^2$  does not change the Hopf invariant of a map  $S^3 \rightarrow S^2$ . The same is true for  $d_3(\xi)$ , since  $c_1(X, J) = -c_1(X, -J)$ . This implies that on  $S^3$  any oriented contact structure is (co-)orientation-reversingly isotopic to itself. For  $\xi_{\text{st}}$  as in (1) such an isotopy is given by a rotation through an angle  $\pi$  in the  $x_1x_2$ -plane; this isotopy carries over to suitable surgery descriptions of the overtwisted contact structures.

We shall also need the following formula [5, Cor. 3.6] for the  $d_3$ -invariant of a contact manifold  $(Y, \xi)$  with  $c_1(\xi)$  torsion that is obtained by contact  $(\pm 1)$ -surgery in the sense of [2] along the oriented components of a Legendrian link  $\mathbb{L} = \mathbb{L}_+ \sqcup \mathbb{L}_-$ , all of which have non-vanishing Thurston–Bennequin invariant. In this situation,

$$(3) \quad d_3(\xi) = \frac{1}{4}(c^2 - 3\sigma(X) - 2\chi(X)) + q;$$

here  $q$  denotes the number of components of  $\mathbb{L}_+$ , and  $c \in H^2(X)$  is the cohomology class determined by  $c(\Sigma_i) = \text{rot}(L_i)$  for each  $L_i \subset \mathbb{L}$ , where  $\Sigma_i \subset X$  is the oriented surface obtained by gluing a Seifert surface of  $L_i$  with the core disc of the corresponding handle.

When we view  $S^3$  as the unit sphere in the quaternions, a natural trivialisation of  $TS^3$  is provided by the basis  $\mathbf{i}p, \mathbf{j}p, \mathbf{k}p$  of  $T_pS^3$ ,  $p \in S^3$ . With this choice we have  $h(\xi_{\text{st}}) = 0$ , since  $\xi_{\text{st},p}$  is spanned by  $\mathbf{j}p$  and  $\mathbf{k}p$ , so the Gauß map  $p \mapsto \mathbf{i}p$  of  $\xi_{\text{st}}$  is the constant map with respect to this trivialisation. This choice is understood in the following lemma.

**Lemma 2.2.** *The Hopf invariant  $h$  and the  $d_3$ -invariant of oriented tangent 2-plane fields on  $S^3$  are related by  $d_3 = -h - \frac{1}{2}$ .*

*Proof.* The standard contact structure  $\xi_{\text{st}}$  may be regarded as the complex tangencies of  $S^3 \subset \mathbb{C}^2$ , and the unit ball in  $\mathbb{C}^2$  constitutes an almost complex filling. Formula (2) then yields  $d_3(\xi_{\text{st}}) = -\frac{1}{2}$ , so the claimed relation between  $h$  and  $d_3$  holds in this case.

In order to verify the relation in general, we consider the effect of a  $\pi$ -Lutz twist along a transverse knot  $K$  in  $(S^3, \xi_{\text{st}})$ . As shown in [15, p. 147] or [10, p. 114], the resulting contact structure  $\xi_K$  satisfies

$$h(\xi_K) = \text{sl}(K),$$

where  $\text{sl}(K)$  denotes the self-linking number of  $K$ .

Let  $L_{-1}$  be the standard Legendrian unknot in  $(S^3, \xi_{\text{st}})$  with  $\text{tb}(L_{-1}) = -1$  and  $\text{rot}(L_{-1}) = 0$ . Its positive transverse push-off  $K_{-1}$ , by [15, Prop. 3.5.36], has self-linking number

$$\text{sl}(K_{-1}) = \text{tb}(L_{-1}) - \text{rot}(L_{-1}) = -1.$$

Write  $\xi_{-1}$  for the contact structure obtained by a Lutz twist along  $K_{-1}$ , so that  $h(\xi_{-1}) = -1$ . According to [6], performing a Lutz twist along  $K_{-1}$  has the same effect as contact (+1)-surgeries along  $L_{-1}$  and its Legendrian push-off with two additional negative stabilisations.

Thus, the linking matrix of this surgery diagram is

$$M = \begin{pmatrix} 0 & -1 \\ -1 & 2 \end{pmatrix},$$

and the vector of rotation numbers equals  $\underline{\text{rot}} = (0, -2)^t$ . The number  $c^2$  is computed as  $\mathbf{x}^t M \mathbf{x}$ , where  $\mathbf{x}$  is the solution of  $M \mathbf{x} = \underline{\text{rot}}$ . This yields  $c^2 = 0$ , and observing that  $\sigma = 0$  and  $\chi = 3$  we find that the contact structure  $\xi_{-1}$  satisfies  $d_3(\xi_{-1}) = \frac{1}{2}$ , which verifies the lemma for  $\xi_{-1}$ .

Similarly, we can find a Legendrian knot  $L_1$  in  $(S^3, \xi_{\text{st}})$  with  $\text{tb}(L_1) = 1$  and  $\text{rot}(L_1) = 0$ , e.g. a suitable Legendrian realisation of the right-handed trefoil knot [14, Figure 8]. Its positive transverse push-off  $K_1$  has  $\text{sl}(K_1) = 1 - 0 = 1$ , so a Lutz twist along  $K_1$  yields a contact structure  $\xi_1$  with  $h(\xi_1) = 1$ . The corresponding surgery picture, by a computation analogous to the one above, allows us to compute  $d_3(\xi_1) = -\frac{3}{2}$ , which accords with our claim.

Under the disjoint (and unlinked) union of copies of  $K_{-1}$  and  $K_1$ , the self-linking number and hence the Hopf invariant of the contact structure obtained by Lutz twists is additive. The Lutz twists along such a disjoint union amounts to a connected sum of the contact manifolds obtained by individual Lutz twists. On the other hand, the  $d_3$ -invariant of the connected sum of two contact structures  $\xi, \xi'$  on  $S^3$  is given by

$$d_3(\xi \# \xi') = d_3(\xi) + d_3(\xi') + \frac{1}{2},$$

see [5, Lemma 4.2]. The formula  $d_3 = -h - \frac{1}{2}$  now follows in full generality.  $\square$

Since we are mostly working with surgery diagrams, we shall in the sequel denote the overtwisted contact structures on  $S^3$  by their  $d_3$ -invariant, that is, we shall write  $\xi_d$  for the unique overtwisted contact structure with  $d_3(\xi_d) = d \in \mathbb{Z} + \frac{1}{2}$ . There can be no confusion with the notation  $\xi_{\pm 1}$ , using the Hopf invariant, in the present section, since the values of the two invariants range over disjoint sets.

### 3. THE LINK COMPLEMENT

The classification of tight contact structures on  $T^2 \times [0, 1]$  is due to Giroux [21] and Honda [24]. In this section we use their results to find the number of tight contact structures on the complement of a Legendrian Hopf link  $L_0 \sqcup L_1$ , in terms of the Thurston–Bennequin invariant of the link components.

We think of  $S^3$  as being decomposed into two solid tori  $V_0, V_1$ , chosen as tubular neighbourhoods of  $L_0, L_1$ , respectively, and a thickened torus  $T^2 \times [0, 1]$ , i.e.

$$S^3 = V_0 \cup_{\partial V_0 = T^2 \times \{0\}} T^2 \times [0, 1] \cup_{T^2 \times \{1\} = \partial V_1} V_1.$$

We write  $\mu_i, \lambda_i$  for meridian and longitude on  $\partial V_i$ , and we take the gluing in the decomposition above to be given by

$$\begin{aligned} \mu_0 &= S^1 \times \{*\} \times \{0\}, \\ \lambda_0 &= \{*\} \times S^1 \times \{0\}, \\ \mu_1 &= \{*\} \times S^1 \times \{1\}, \\ \lambda_1 &= S^1 \times \{*\} \times \{1\}. \end{aligned}$$

Given a Legendrian Hopf link  $L_0 \sqcup L_1$  with  $\mathfrak{tb}(L_i) =: \mathfrak{t}_i$ ,  $i = 0, 1$ , we can choose  $V_i$  as a standard neighbourhood of  $L_i$ , meaning that  $\partial V_i$  is a convex surface with two dividing curves of slope  $1/\mathfrak{t}_i$  with respect to the identification of  $\partial V_i$  with  $\mathbb{R}^2/\mathbb{Z}^2$  defined by  $(\mu_i, \lambda_i)$ .

On  $T^2 \times [0, 1]$  we measure slopes on the  $T^2$ -factor with respect to  $(\mu_0, \lambda_0)$ . This means that in the described situation we are dealing with a contact structure on  $T^2 \times [0, 1]$  with convex boundary, two dividing curves on either boundary component, of slope  $s_0 = 1/\mathfrak{t}_0$  on  $T^2 \times \{0\}$ , and of slope  $s_1 = \mathfrak{t}_1$  on  $T^2 \times \{1\}$ . Recall that a contact structure on  $T^2 \times [0, 1]$  with these boundary conditions is called *minimally twisting* if every convex torus parallel to the boundary has slope between  $s_1$  and  $s_0$ .

The following proposition covers all possible pairs  $(\mathfrak{t}_0, \mathfrak{t}_1)$ , possibly after exchanging the roles of  $L_0$  and  $L_1$ .

**Proposition 3.1.** *Up to an isotopy fixing the boundary, the number  $N = N(\mathfrak{t}_0, \mathfrak{t}_1)$  of tight, minimally twisting contact structures on  $T^2 \times [0, 1]$  with convex boundary, two dividing curves on either boundary component of slope  $s_0 = 1/\mathfrak{t}_0$  and  $s_1 = \mathfrak{t}_1$ , respectively, is as follows.*

- (a1) If  $\mathfrak{t}_0, \mathfrak{t}_1 < 0$ , excluding the case  $\mathfrak{t}_0 = \mathfrak{t}_1 = -1$ , we have  $N = \mathfrak{t}_0 \mathfrak{t}_1$ .
- (a2) If  $\mathfrak{t}_0 = \mathfrak{t}_1 = -1$ , there is a unique structure up to diffeomorphism, and an integral family (distinguished by a holonomy map) up to isotopy.
- (b1) If  $\mathfrak{t}_0 < 0$  and  $\mathfrak{t}_1 \geq 2$ , then  $N = 2|\mathfrak{t}_0 - 1|$ .
- (b2) If  $\mathfrak{t}_0 < 0$  and  $\mathfrak{t}_1 = 1$ , then  $N = |\mathfrak{t}_0 - 2|$ .
- (c1) If  $\mathfrak{t}_0 = \mathfrak{t}_1 = 1$ , there is a unique structure up to diffeomorphism, and an integral family (distinguished by a holonomy map) up to isotopy.
- (c2)  $N(2, 1) = 2$ ,  $N(3, 1) = 3$ , and  $N(2, 2) = 4$ .
- (c3) For all  $\mathfrak{t}_0 \geq 4$  we have  $N(\mathfrak{t}_0, 1) = 4$ ; for all  $\mathfrak{t}_0 \geq 3$  we have  $N(\mathfrak{t}_0, 2) = 6$ .

- (c4) For all  $\mathfrak{t}_0 \geq \mathfrak{t}_1 \geq 3$ , we have  $N(\mathfrak{t}_0, \mathfrak{t}_1) = 8$ .  
 (d) For all  $\mathfrak{t}_1 \in \mathbb{Z}$ , we have  $N(0, \mathfrak{t}_1) = 2$ .

*Proof.* In all cases, we need to normalise the slopes by applying an element of  $\text{Diff}^+(T^2) \simeq \text{SL}(2, \mathbb{Z})$  to  $T^2 \times [0, 1]$  such that the slope on  $T^2 \times \{0\}$  becomes  $s'_0 = -1$ , and on  $T^2 \times \{1\}$  we have  $s'_1 \leq -1$ . If  $s'_1 < -1$ , the number  $N$  is found from a continuous fraction expansion

$$s'_1 = r_0 - \frac{1}{r_1 - \frac{1}{r_2 - \cdots - \frac{1}{r_k}}}$$

with all  $r_i < -1$  as

$$(4) \quad N = |(r_0 + 1) \cdots (r_{k-1} + 1)r_k|,$$

see [24, Theorem 2.2(2)]. The vector  $\begin{pmatrix} x \\ y \end{pmatrix}$  stands for the curve  $x\mu_0 + y\lambda_0$ , with slope  $y/x$ .

(a1) We have

$$\begin{pmatrix} 0 & 1 \\ -1 & \mathfrak{t}_0 - 1 \end{pmatrix} \begin{pmatrix} \mathfrak{t}_0 \\ 1 \end{pmatrix} = \begin{pmatrix} 1 \\ -1 \end{pmatrix} \quad \text{and} \quad \begin{pmatrix} 0 & 1 \\ -1 & \mathfrak{t}_0 - 1 \end{pmatrix} \begin{pmatrix} 1 \\ \mathfrak{t}_1 \end{pmatrix} = \begin{pmatrix} \mathfrak{t}_1 \\ \mathfrak{t}_0\mathfrak{t}_1 - \mathfrak{t}_1 - 1 \end{pmatrix}.$$

This means

$$(5) \quad s'_1 = \mathfrak{t}_0 - 1 - \frac{1}{\mathfrak{t}_1}.$$

If  $\mathfrak{t}_1 \leq -2$ , this is a continued fraction expansion  $[\mathfrak{t}_0 - 1, \mathfrak{t}_1]$  as required by [24], and by (4) we have  $N = \mathfrak{t}_0\mathfrak{t}_1$ . If  $\mathfrak{t}_1 = -1$ , but  $\mathfrak{t}_2 \leq -2$ , we have the continued fraction expansion  $s'_1 = [\mathfrak{t}_0]$ , and again this gives  $|\mathfrak{t}_0| = \mathfrak{t}_0\mathfrak{t}_1$  structures.

(a2) If  $\mathfrak{t}_0 = \mathfrak{t}_1 = -1$ , we can apply the same transformation as in (a), and we are then in the situation  $s'_0 = s'_1 = -1$  of [24, Theorem 2.2(4)], cf. [13, Theorem 6.1], which gives the claimed number.

(b1) Using the transformation as in (a), we find the same  $s'_1 < -1$  as in (5), but this is not, as it stands, a continued fraction expansion of the required form. From the continued fraction expansion

$$(6) \quad -\frac{p+1}{p} = \underbrace{[-2, \dots, -2]}_p \quad \text{for } p \in \mathbb{N}$$

we find

$$\mathfrak{t}_0 - 1 - \frac{1}{\mathfrak{t}_1} = \mathfrak{t}_0 - \frac{\mathfrak{t}_1 + 1}{\mathfrak{t}_1} = [\mathfrak{t}_0 - 2, \underbrace{-2, \dots, -2}_{\mathfrak{t}_1 - 1}].$$

By (4) this yields  $N = 2|\mathfrak{t}_0 - 1|$ .

(b2) In this case the transformed slope is  $s'_1 = \mathfrak{t}_0 - 2$ , so the continued fraction expansion is  $[\mathfrak{t}_0 - 2]$ , giving us  $|\mathfrak{t}_0 - 2|$  structures by (4).

(c) We consider the transformation

$$\begin{pmatrix} 1 & 1 - \mathfrak{t}_0 \\ -2 & -1 + 2\mathfrak{t}_0 \end{pmatrix} \begin{pmatrix} \mathfrak{t}_0 \\ 1 \end{pmatrix} = \begin{pmatrix} 1 \\ -1 \end{pmatrix}$$

and

$$\begin{pmatrix} 1 & 1 - \mathfrak{t}_0 \\ -2 & -1 + 2\mathfrak{t}_0 \end{pmatrix} \begin{pmatrix} 1 \\ \mathfrak{t}_1 \end{pmatrix} = \begin{pmatrix} 1 + \mathfrak{t}_1 - \mathfrak{t}_0\mathfrak{t}_1 \\ -2 - \mathfrak{t}_1 + 2\mathfrak{t}_0\mathfrak{t}_1 \end{pmatrix}.$$

This gives

$$s'_1 = \frac{-2 - \mathfrak{t}_1 + 2\mathfrak{t}_0\mathfrak{t}_1}{1 + \mathfrak{t}_1 - \mathfrak{t}_0\mathfrak{t}_1} = -2 + \frac{\mathfrak{t}_1}{1 + \mathfrak{t}_1 - \mathfrak{t}_0\mathfrak{t}_1},$$

which is smaller than  $-1$  for  $\mathfrak{t}_0 \geq \mathfrak{t}_1 > 0$ , except in the cases  $(\mathfrak{t}_0, \mathfrak{t}_1) = (1, 1)$  and  $(\mathfrak{t}_0, \mathfrak{t}_1) = (2, 1)$ , when  $s'_1 = -1$  or  $s'_1 = \infty$ , respectively.

(c1) For  $(\mathfrak{t}_0, \mathfrak{t}_1) = (1, 1)$  the argument is now as in the case (a2).

(c2) For  $(\mathfrak{t}_0, \mathfrak{t}_1) = (2, 2)$  we have  $s'_1 = -4$ , which by (4) gives  $N = 4$ . For  $\mathfrak{t}_1 = 1$  and  $\mathfrak{t}_0 = 3$  we have  $s'_1 = -3$ , and hence  $N = 3$ . For  $(\mathfrak{t}_0, \mathfrak{t}_1) = (2, 1)$  we need to choose a different transformation to obtain  $s'_1 \leq -1$ . Such a transformation is given by

$$\begin{pmatrix} 2 & -3 \\ -3 & 5 \end{pmatrix} \begin{pmatrix} 2 \\ 1 \end{pmatrix} = \begin{pmatrix} 1 \\ -1 \end{pmatrix} \quad \text{and} \quad \begin{pmatrix} 2 & -3 \\ -3 & 5 \end{pmatrix} \begin{pmatrix} 1 \\ 1 \end{pmatrix} = \begin{pmatrix} -1 \\ 2 \end{pmatrix},$$

which yields  $s'_1 = -2$  and hence  $N = 2$ .

(c3) For  $\mathfrak{t}_0 \geq 4$ , we have the continued fraction expansion

$$s'_1 = \frac{-3 + 2\mathfrak{t}_0}{2 - \mathfrak{t}_0} = -3 + \frac{\mathfrak{t}_0 - 3}{\mathfrak{t}_0 - 2} = -3 - \frac{1}{-\frac{\mathfrak{t}_0 - 2}{\mathfrak{t}_0 - 3}} = [-3, \underbrace{-2, \dots, -2}_{\mathfrak{t}_0 - 3}]$$

by (6), which by (4) yields  $N = 2 \cdot 2 = 4$ .

For  $\mathfrak{t}_0 \geq 3$  and  $\mathfrak{t}_1 = 2$  we find

$$s'_1 = \frac{4\mathfrak{t}_0 - 4}{3 - 2\mathfrak{t}_0} = [-3, \underbrace{-2, \dots, -2}_{\mathfrak{t}_0 - 3}, -3].$$

In order to verify this continued fraction expansion, one may observe that

$$(7) \quad \underbrace{[-2, \dots, -2]_p}_{p} - 3 = -\frac{2p + 3}{2p + 1},$$

which is easily proved by induction. Given this expansion for  $s'_1$ , with (4) we obtain  $N = 2 \cdot 3 = 6$ .

(c4) The formula (7) can be generalised to

$$\underbrace{[-2, \dots, -2]_p}_{p}, \frac{a}{b} := -2 - \frac{1}{-2 - \frac{1}{-2 - \dots - \frac{1}{a/b}}} = -\frac{(p+1)a + pb}{pa + (p-1)b}.$$

It is then straightforward to verify that

$$s'_1 = \frac{-2 - \mathfrak{t}_1 + 2\mathfrak{t}_0\mathfrak{t}_1}{1 + \mathfrak{t}_1 - \mathfrak{t}_0\mathfrak{t}_1} = [-3, \underbrace{-2, \dots, -2}_{\mathfrak{t}_0 - 3}, -3, \underbrace{-2, \dots, -2}_{\mathfrak{t}_1 - 2}].$$

With (4) this yields

$$N = |(-3 + 1) \cdot (-3 + 1) \cdot (-2)| = 8.$$

(d1) For  $\mathfrak{t}_0 = 0$  and  $\mathfrak{t}_1 > 0$  we use the transformation

$$\begin{pmatrix} 0 & 1 \\ -1 & -1 \end{pmatrix} \begin{pmatrix} 0 \\ 1 \end{pmatrix} = \begin{pmatrix} 1 \\ -1 \end{pmatrix} \quad \text{and} \quad \begin{pmatrix} 0 & 1 \\ -1 & -1 \end{pmatrix} \begin{pmatrix} 1 \\ \mathfrak{t}_1 \end{pmatrix} = \begin{pmatrix} \mathfrak{t}_1 \\ -1 - \mathfrak{t}_1 \end{pmatrix},$$



giving us

$$s'_1 = -\frac{\mathfrak{t}_1 + 1}{\mathfrak{t}_1} = \underbrace{[-2, \dots, -2]}_{\mathfrak{t}_1}$$

by (6), and hence  $N = 2$  by (4).

(d2) For  $\mathfrak{t}_0 = 0$  and  $\mathfrak{t}_1 < 0$ , the transformation

$$\begin{pmatrix} -\mathfrak{t}_1 + 1 & 1 \\ \mathfrak{t}_1 - 2 & -1 \end{pmatrix} \begin{pmatrix} 0 \\ 1 \end{pmatrix} = \begin{pmatrix} 1 \\ -1 \end{pmatrix} \quad \text{and} \quad \begin{pmatrix} -\mathfrak{t}_1 + 1 & 1 \\ \mathfrak{t}_1 - 2 & -1 \end{pmatrix} \begin{pmatrix} 1 \\ \mathfrak{t}_1 \end{pmatrix} = \begin{pmatrix} 1 \\ -2 \end{pmatrix}$$

gives us  $s'_1 = -2$ , and hence  $N = 2$  by (4).

(d3) For  $\mathfrak{t}_0 = \mathfrak{t}_1 = 0$  we use the transformation

$$\begin{pmatrix} 1 & 1 \\ -2 & -1 \end{pmatrix} \begin{pmatrix} 0 \\ 1 \end{pmatrix} = \begin{pmatrix} 1 \\ -1 \end{pmatrix} \quad \text{and} \quad \begin{pmatrix} 1 & 1 \\ -2 & -1 \end{pmatrix} \begin{pmatrix} 1 \\ 0 \end{pmatrix} = \begin{pmatrix} 1 \\ -2 \end{pmatrix}.$$

Once again, this yields  $s'_1 = -2$  and  $N = 2$ . □

When a tight contact structure on  $T^2 \times [0, 1]$  is not minimally twisting, one can associate with it a natural number, called the  $\pi$ -*twisting in the  $[0, 1]$ -direction* [24, Section 2.2.1], or simply *twisting*.

There is also a notion of torsion for contact structures, introduced by Giroux [19, 20]. Let  $(M, \xi)$  be a contact 3-manifold and  $[T]$  an isotopy class of embedded 2-tori in  $M$ . Then the  $\pi$ -*torsion* (or simply *torsion*) of  $(M, \xi)$  is the supremum of  $n \in \mathbb{N}_0$  for which there is a contact embedding of

$$(T^2 \times [0, 1], \ker(\sin(n\pi z) dx + \cos(n\pi z) dy))$$

into  $(M, \xi)$ , with  $T^2 \times \{z\}$  being sent to the class  $[T]$ .

As explained in [25, p. 86], the twisting of a contact structure on  $T^2 \times [0, 1]$  equals its torsion with respect to the class  $[T^2 \times \{z\}]$ . For the computation of the torsion, it is assumed that the characteristic foliation on the boundary tori is a non-singular foliation of some rational slope; the twisting is computed for a convex boundary with dividing curves of the same slope, obtained by a slight perturbation of the boundary tori.

The following isotopy classification can be found in [24, Theorem 2.2]. The diffeomorphism classification for  $s_1 = -1$  can be deduced from the explicit description of these structures in [24, Lemma 5.2]. The fact that in all other cases there are two structures even up to diffeomorphism is a consequence of having two Legendrian realisations of Hopf links whose complement has such boundary data, see Section 7.

**Proposition 3.2.** *Up to an isotopy fixing the boundary, the number of tight contact structures on  $T^2 \times [0, 1]$  with convex boundary, two dividing curves on either boundary of slope  $s_0 = -1$  and  $s_1 \leq -1$  and positive twisting  $n \in \mathbb{N}$ , equals two for each  $n$ . Up to a diffeomorphism fixing the boundary, the number is likewise two, except in the case  $s_1 = -1$ , when it equals one.* □

**Remark 3.3.** The two contact structures with a given positive twisting and the same boundary data differ only by the choice of coorientation. For  $s_1 = -1$ , a diffeomorphism changing the coorientation is given by  $T^2 \rightarrow T^2$ ,  $(x, y) \mapsto (-y, x)$ .

By transforming the slopes as in the proof of Proposition 3.1, we see that Proposition 3.2 applies likewise to contact structures with positive twisting and any combination of boundary slopes  $s_0 = 1/\mathfrak{t}_0$  and  $s_1 = \mathfrak{t}_1$ .

4. HOPF LINKS IN  $(S^3, \xi_{\text{st}})$ 

The classification of Legendrian Hopf links in the tight contact structure  $\xi_{\text{st}}$  on  $S^3$ , up to Legendrian isotopy, was carried out in [3] as part of a more general study of Legendrian cable links. As shown there, these links are classified by their classical invariants, and the range of these invariants is the same for each component as for a single Legendrian unknot, i.e. the Thurston–Bennequin invariants of the two components can be any pair of negative integers, and for  $\text{tb}(L_i) = -m$  the rotation number of  $L_i$  can take any value in the set

$$\{-m + 1, -m + 3, \dots, m - 3, m - 1\}.$$

Explicit realisations are given by stabilising the components of the Hopf link shown (in the front projection) in Figure 1, where the two components have  $\text{tb} = -1$  and  $\text{rot} = 0$ .

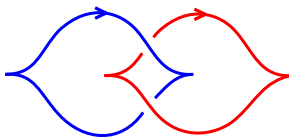


FIGURE 1. Legendrian Hopf link in  $(S^3, \xi_{\text{st}})$ .

Here is an alternative proof of this result. For given values of  $\tau_0, \tau_1 < 0$ , we have  $\tau_0\tau_1$  explicit realisations in  $(S^3, \xi_{\text{st}})$ , which is the maximal number possible by Proposition 3.1 (a). There are no realisations in  $(S^3, \xi_{\text{st}})$  with one of the  $\tau_i$  being non-negative, since Legendrian unknots in  $(S^3, \xi_{\text{st}})$  satisfy  $\text{tb} < 0$  by the Bennequin inequality [15, Theorem 4.6.36]. Also, there are no realisations with twisting in the complement, since this would force the corresponding contact structure on  $S^3$  to be overtwisted.

This proves part (a) of Theorem 1.2.

## 5. STRONGLY EXCEPTIONAL HOPF LINKS

In this section we classify the Legendrian realisations of the Hopf link in overtwisted contact structures whose link complement is tight and minimally twisting.

**5.1. Kirby moves.** We begin with some examples of Kirby diagrams of the Hopf link that will be relevant in several cases of this classification.

**Lemma 5.1.** (i) *The oriented link  $L_0 \sqcup L_1$  in the surgery diagram shown in the first line of Figure 2 is a positive or negative Hopf link in  $S^3$ , depending on  $n$  being even or odd.*

(ii) *The same is true for the link shown in the first line of Figure 5.*

(iii) *The oriented link  $L_0 \sqcup L_1$  on the top left of Figure 3 is a positive Hopf link; the same holds for the links in Figures 4 and 6.*

*Proof.* For (i) and (iii) this follows from the Kirby moves shown in the corresponding figure. For (ii) we observe that the Kirby moves in Figure 5 reduce this to the situation in (i), with  $n$  replaced by  $n + 2$ . (The roles of  $L_0$  and  $L_1$  are exchanged in this diagram compared with Figure 2; this choice conforms with the Legendrian realisations discussed below.)  $\square$

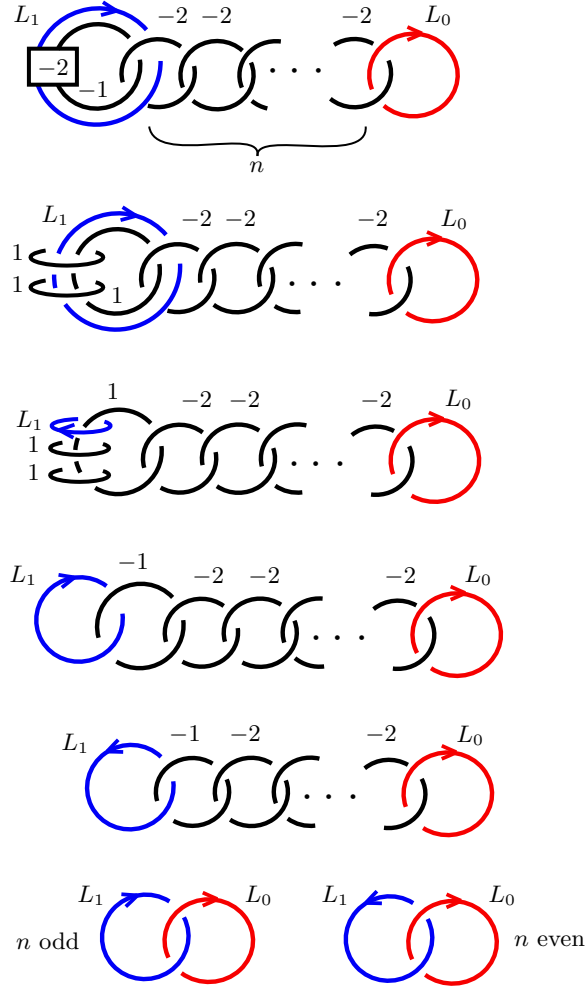


FIGURE 2. Kirby diagram of a Hopf link I.

**5.2. Computing the invariants.** We are going to describe Legendrian realisations  $L_0 \sqcup L_1$  of the Hopf link in  $(S^3, \xi_d)$  as front projections in a contact surgery diagram for this contact manifold. Here we briefly summarise how to compute the classical invariants in this setting.

We number the Legendrian knots in the contact surgery diagram as  $K_1, \dots, K_n$  and choose auxiliary orientations on them. Write  $M$  for the corresponding linking matrix, with the diagonal entries given by the topological surgery framing. Given the presentation of a Legendrian knot  $L_i$  in the surgery diagram, we form the extended linking matrix

$$M_i = \left( \begin{array}{c|ccc} 0 & \text{lk}(L_i, K_1) & \cdots & \text{lk}(L_i, K_n) \\ \hline \text{lk}(L_i, K_1) & & & \\ \vdots & & M & \\ \text{lk}(L_i, K_n) & & & \end{array} \right).$$

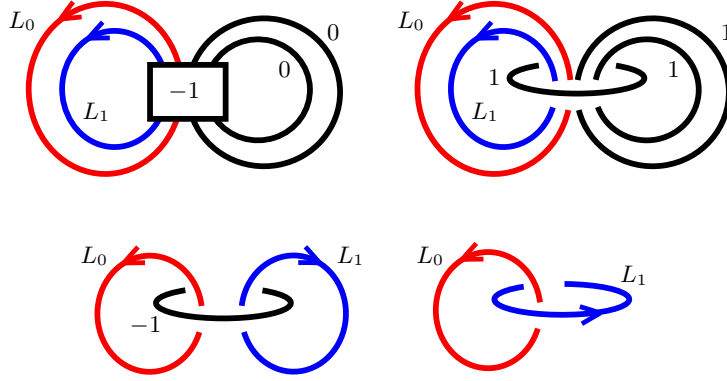


FIGURE 3. Kirby diagram of a Hopf link II.

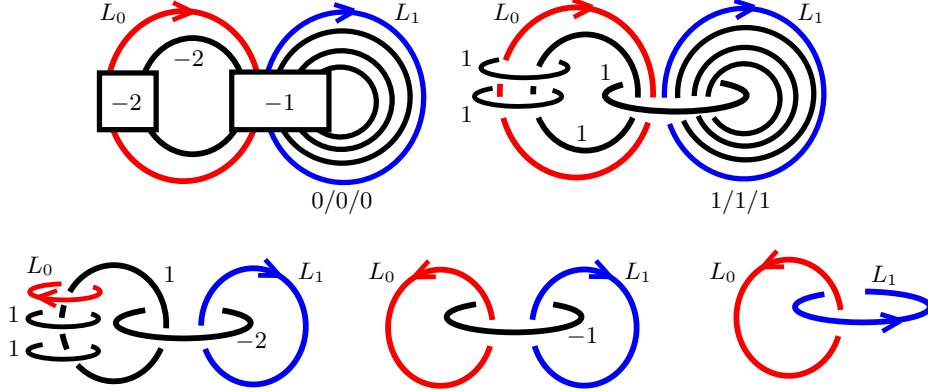


FIGURE 4. Kirby diagram of a Hopf link III.

5.2.1. *Thurston–Bennequin invariant.* Write  $\text{tb}_i$  for the Thurston–Bennequin invariant of  $L_i$  as a knot in  $(S^3, \xi_{\text{st}})$ , before performing the contact surgeries along  $K_1, \dots, K_n$ . Then, as shown in [27, Lemma 6.6], the Thurston–Bennequin invariant  $\text{tb}(L_i)$  in the contact structure on  $S^3$  obtained by contact surgeries along  $K_1, \dots, K_n$  is

$$(8) \quad \text{tb}(L_i) = \text{tb}_i + \frac{\det M_i}{\det M}.$$

Alternatively, one can keep track of the contact framing of  $L_i$  during the topological Kirby moves that turn the given surgery diagram into the empty diagram, and  $L_0 \sqcup L_1$  into the standard Hopf link in this empty diagram for  $S^3$ .

5.2.2. *Rotation number.* By  $\text{rot}_i$  we denote the rotation number of  $L_i$  before the surgery. Write

$$\underline{\text{rot}} = (\text{rot}(K_1), \dots, \text{rot}(K_n))$$

for the vector of rotation numbers of the surgery knots, and

$$\underline{\text{lk}}_i = (\text{lk}(L_i, K_1), \dots, \text{lk}(L_i, K_n))$$

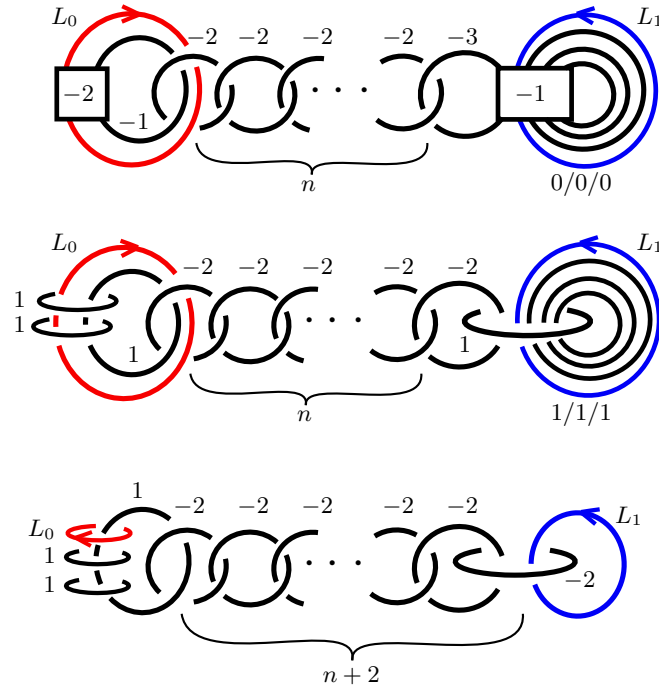


FIGURE 5. Kirby diagram of a Hopf link IV.

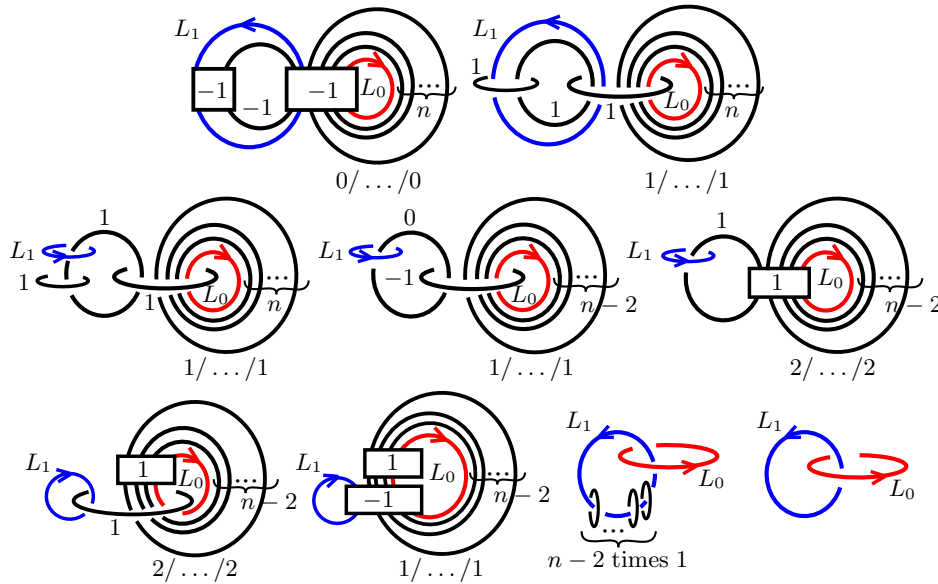


FIGURE 6. Kirby diagram of a Hopf link V.

for the vector of linking numbers. Then, again by [27, Lemma 6.6], the rotation number  $\text{rot}(L_i)$  of  $L_i$  after the surgery is

$$(9) \quad \text{rot}(L_i) = \text{rot}_i - \langle \underline{\text{rot}}, M^{-1} \underline{1k}_i \rangle.$$

5.2.3. *The  $d_3$ -invariant.* In order to compute the  $d_3$ -invariant with formula (3), we need to read off  $c^2, \sigma$  and  $\chi$  from the surgery diagram. Each surgery knot corresponds to the attaching of a 2-handle, hence the Euler characteristic of the handlebody is  $\chi = 1 + n$ .

The signature  $\sigma$  can be determined as the signature of the linking matrix  $M$ . More topologically, one can determine  $\sigma$  from the Kirby moves for showing that the surgery diagram actually gives a description of  $S^3$ . These Kirby moves involve handle slides and the blowing down of  $(\pm 1)$ -framed unknots. The signature  $\sigma$  equals the number of these blow-downs, counted with sign, minus the number of  $(\pm 1)$ -framed unknots that may have been introduced into the Kirby diagram to replace twisting boxes.

The computation of  $c^2$  has been explained in [5]. Find the solution vector  $\mathbf{x}$  of the equation  $M\mathbf{x} = \underline{\mathbf{rot}}$ ; then  $c^2 = \mathbf{x}^t M \mathbf{x} = \langle \mathbf{x}, \underline{\mathbf{rot}} \rangle$ .

5.3. **Detecting exceptional links.** In order to decide whether a Legendrian knot presented in a contact surgery diagram of  $(S^3, \xi)$  is exceptional, we first need to verify that the ambient contact structure  $\xi$  is overtwisted. If the  $d_3$ -invariant differs from that of the standard structure  $\xi_{\text{st}}$ , that is, if  $d_3(\xi) \neq -\frac{1}{2}$ , this is obvious. In the case where  $d_3(\xi) = -\frac{1}{2}$ , it suffices to find a Legendrian knot in the surgered manifold that violates the Bennequin inequality [15, Theorem 4.6.36] for Legendrian knots in tight contact 3-manifolds. In our examples, one of  $L_0$  or  $L_1$  will have this property.

Secondly, we need to establish that the contact structure on the link complement  $S^3 \setminus (L_0 \sqcup L_1)$  is tight. The method we use is to perform contact surgeries on  $L_0$  and  $L_1$ , perhaps also on Legendrian push-offs of these knots, such that the resulting contact manifold is tight. If there had been an overtwisted disc in the complement of  $L_0 \sqcup L_1$ , this would persist after the surgery.

Here we always employ the cancellation lemma from [2], cf. [15, Proposition 6.4.5], which says that a contact  $(-1)$ -surgery and a contact  $(+1)$ -surgery along a Legendrian knot and its Legendrian push-off, respectively, cancel each other. Thus, if by contact  $(-1)$ -surgeries along  $L_0$  and  $L_1$  we can cancel all contact  $(+1)$ -surgeries in the surgery diagram, and thus obtain a Stein fillable and hence tight contact 3-manifold, the Legendrian Hopf link will have been exceptional. In fact, in this case there is also no torsion in the complement, so the link is strongly exceptional.

5.4. **Exceptional unknots.** The individual components  $L_0, L_1$  of an exceptional Hopf link may be exceptional or loose. Which of the two cases occurs for either component can be decided by referring to the classification of exceptional unknots due to Eliashberg and Fraser [10], cf. [17], which we recall here.

**Theorem 5.2** (Eliashberg–Fraser). *Exceptional unknots can only be realised in the contact structure  $\xi_{1/2}$  on  $S^3$ . Up to coarse equivalence, they are classified by their classical invariants, which can take the values  $(\mathbf{tb}, \mathbf{rot}) = (n, \pm(n-1))$ ,  $n \in \mathbb{N}$ .*

5.5. **Legendrian realisations.** We now turn our attention to Legendrian realisations of the Hopf link in terms of Legendrian surgery diagrams. The invariants of these realisations are collected in Table 2 in Section 9.

5.5.1. *Case (b1).* As we shall explain, Figure 7 shows the  $2|\mathbf{t}_0 - 1|$  Legendrian realisations of the Hopf link with  $\mathbf{t}_0 < 0$  and  $\mathbf{t}_1 \geq 2$ . The numbers  $k, \ell \in \mathbb{N}_0$  may be chosen subject to the condition  $-\mathbf{t}_0 = k + \ell$ , and  $n \in \mathbb{N}_0$  is determined by



By expanding this matrix along the first row and column, we find  $\det M_0^{(n)} = -\det M^{(n-1)} = (-1)^{n+1}$ , too. Hence, by (8),

$$\mathbf{tb}(L_0) = \mathbf{tb}_0 + \frac{\det M_0}{\det M} = -(k + \ell + 1) + 1 = -(k + \ell).$$

When  $L_0$  is oriented clockwise, we have  $\mathbf{rot}_0 = \ell - k$ . The first row of  $M^{-1}$  is

$$(-(n+1), n, -(n-1), \dots, (-1)^{n+1} \cdot 1).$$

The vector of rotation numbers of the surgery curves is  $\mathbf{rot} = (1, 0, \dots, 0)^\mathbf{t}$ , and the vector of linking numbers of  $L_0$  with the surgery curves is  $\mathbf{lk} = (0, \dots, 0, -1)^\mathbf{t}$ . With (9) this yields

$$\mathbf{rot}(L_0) = \mathbf{rot}_0 - \left\langle \begin{pmatrix} 1 \\ 0 \\ \vdots \\ 0 \\ 0 \end{pmatrix}, M^{-1} \begin{pmatrix} 0 \\ 0 \\ \vdots \\ 0 \\ -1 \end{pmatrix} \right\rangle = \ell - k - (-1)^n.$$

The invariants of  $L_1$  have been computed in [17, Section 9.1]. With the orientation that makes  $L_0 \sqcup L_1$  a positive Hopf link (clockwise for  $n$  even, counterclockwise for  $n$  odd; see Lemma 5.1 (i)), the invariants are

$$\mathbf{tb}(L_1) = n + 2 \quad \text{and} \quad \mathbf{rot}(L_1) = -(-1)^n(n + 1).$$

The surgery diagram is equivalent to surgery along  $n + 1$  unlinked  $(-1)$ -framed unknots. This gives  $\sigma = -(n + 1)$  and  $\chi = n + 2$ , as can be seen from Figure 2. Moreover, the vector  $\mathbf{x} = M^{-1}\mathbf{rot}$  is the first column (or row) of  $M^{-1}$ , hence  $c^2 = \mathbf{x}^\mathbf{t} M \mathbf{x} = \langle \mathbf{x}, \mathbf{rot} \rangle = -(n + 1)$ . Putting this into formula (3) gives  $d_3(\xi) = 1/2$ . The knot  $L_1$  is one of the exceptional unknots in  $S^3$  described earlier in [10] (see Theorem 5.2) and, in terms of surgery diagrams, in [17]; observe that contact  $(-1)$ -surgery along  $L_1$  cancels the single contact  $(+1)$ -surgery, and hence produces a tight contact 3-manifold. The knot  $L_0$  is loose, since by Theorem 5.2 there are no exceptional realisations of the unknot with these invariants.

5.5.2. *Case (b2).* The  $|\mathbf{t}_0 - 2|$  Legendrian realisations are shown in Figure 8, where both  $L_0$  and  $L_1$  are oriented clockwise, and  $k + \ell = -\mathbf{t}_0 + 1 \geq 2$ ,  $k, \ell \in \mathbb{N}_0$ .

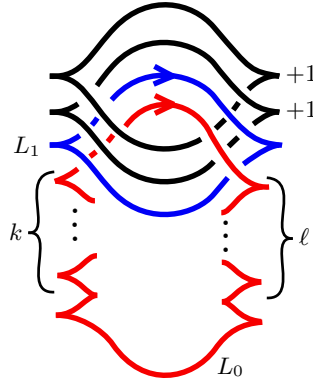


FIGURE 8. Case (b2): Legendrian Hopf links with  $\mathbf{t}_0 < 0$ ,  $\mathbf{t}_1 = 1$ .



The relevant data for the knot  $L_1$  are

$$M = \begin{pmatrix} 0 & -1 \\ -1 & 0 \end{pmatrix} \quad \text{and} \quad M_0 = \begin{pmatrix} 0 & -1 & -1 \\ -1 & 0 & -1 \\ -1 & -1 & 0 \end{pmatrix}.$$

The signature of  $M$  is  $\sigma = 0$ . The vector  $\underline{\text{rot}}$  is the zero vector. This gives  $\text{tb}(L_1) = 1$  and  $\text{rot}(L_1) = 0$ .

The knot  $L_0$  by itself can be viewed as a stabilisation of  $L_1$ . This yields  $\text{tb}(L_0) = 1 - (k + \ell) = \mathfrak{t}_0$  and  $\text{rot}(L_0) = \ell - k$ . So for case (b2) we want  $k + \ell \geq 2$ .

The Kirby moves showing that  $L_0 \sqcup L_1$  is a positive Hopf link in  $S^3$  are shown in Figure 3. The computation of  $d_3 = \frac{1}{2}$  for the contact structure on  $S^3$  after the surgery is straightforward.

Contact  $(-1)$ -surgery along  $L_1$  leaves only a single contact  $(+1)$ -surgery along a  $\text{tb} = -1$  unknot, which produces the tight contact structure on  $S^1 \times S^2$ , see [5, Lemma 4.3]. This shows that  $L_1$  by itself is exceptional. (An alternative surgery picture for  $L_1$  is shown in [17, Figure 3].) The knot  $L_0$  is loose, since by Theorem 5.2 there is no exceptional realisation of the unknot with negative  $\text{tb}$ .

The same arguments, with the same surgery picture, apply when  $k + \ell = 1$ , which gives the subcase  $(\mathfrak{t}_0, \mathfrak{t}_1) = (0, 1)$  of (d). For  $k = \ell = 0$  we obtain case (c1). The only difference with (b2) is that now  $L_0$  is also exceptional, since it is simply a parallel copy of  $L_1$ .

5.5.3. *Case (c2)*. The two realisations with  $(\mathfrak{t}_0, \mathfrak{t}_1) = (2, 1)$  will be described in Section 7.4.1. The three realisations with  $(\mathfrak{t}_0, \mathfrak{t}_1) = (3, 1)$  are shown in Figure 9. The Kirby moves in Figure 4 demonstrate that Figure 9 does indeed depict a Hopf link.

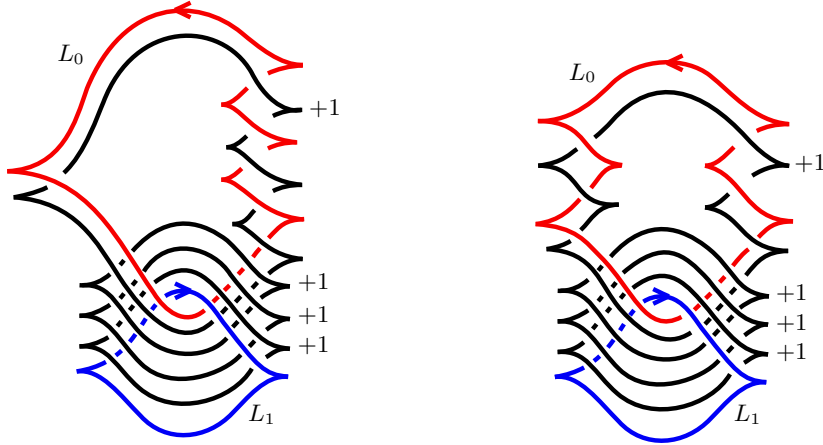


FIGURE 9. Case (c2): Legendrian Hopf links with  $\mathfrak{t}_0 = 3, \mathfrak{t}_1 = 1$ .

The four realisations with  $(\mathfrak{t}_0, \mathfrak{t}_1) = (2, 2)$  are shown in Figure 10. The Kirby moves are similar to the previous case.

The computations of the invariants for the examples in Figures 9 can be found in Section 9; those for Figure 10 are analogous and are left to the reader.

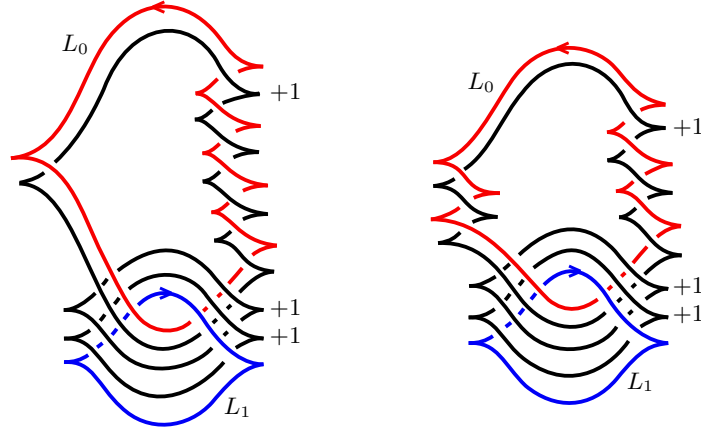


FIGURE 10. Case (c2): Legendrian Hopf links with  $\tau_0 = \tau_1 = 2$ .

5.5.4. *Case (c3)*. Figure 11, where  $n \in \mathbb{N}_0$ , shows the four realisations with  $\tau_0 \geq 4$  and  $\tau_1 = 1$ . The computation of the invariants can be found in Section 9. By Lemma 5.1 (ii) we need to give  $L_0$  and  $L_1$  the same orientation in the plane for  $n$  even; for  $n$  odd, the opposite one.

The six realisations with  $\tau_0 \geq 3$  and  $\tau_1 = 2$  are shown in Figure 12, again with  $n \in \mathbb{N}_0$ ; the invariants are listed in Table 2. For  $n$  odd,  $L_0$  and  $L_1$  are given the same orientation, for  $n$  even, the opposite one. The computation of the invariants is analogous to the other cases. We omit the details.

5.5.5. *Case (c4)*. The eight realisations for each choice of  $\tau_0, \tau_1 \geq 3$  are shown in Figure 13, where  $n, m \in \mathbb{N}_0$ . The Kirby moves showing that these diagrams do indeed depict a Hopf link are similar to those in Figure 2. For  $n + m$  even, one needs to give  $L_0$  and  $L_1$  the same orientation, for  $n + m$  odd, the opposite one. By tracking the contact framing of  $L_0$  and  $L_1$  through these Kirby moves one finds that  $\tau_0 = n + 3$  and  $\tau_1 = m + 3$ . The remaining calculations of the invariants, listed in Table 2, are analogous to the other cases.

**Remark 5.3.** Beware that there is no direct correspondence between the four diagrams in Figure 13 and the four subcases of (c4) listed in Table 2. Rather, the correspondence hinges on the parity of  $m$  and  $n$ . For instance, the realisations with  $d_3 = -\frac{1}{2}$  are given by the first diagram (from the left) for  $m, n$  even, by the second for  $n$  even and  $m$  odd, the third for  $n$  odd and  $m$  even, and the fourth if both  $n$  and  $m$  are odd. The same caveat applies in the case (c3).

5.5.6. *Case (d)*. This is the case with  $\tau_0 = 0$ . Exceptional Legendrian realisations of the Hopf link with  $\tau_1 \leq 0$  are shown in Figure 14, where  $n \geq 2$ . For the computation of the invariants see Section 9. The link components are loose by Theorem 5.2. Examples with  $\tau_1 \geq 2$  are realised by Figure 7 with  $k = \ell = 0$ ; all the arguments from case (b1) apply likewise for this choice of  $k, \ell$ . Figure 8 from case (b2) with  $(k, \ell) \in \{(1, 0), (0, 1)\}$  gives the realisations with  $\tau_1 = 1$ .

5.5.7. *Summary*. In Table 5.5.7 we arrange the strongly exceptional cases from Table 2 with  $\tau_0, \tau_1 \in \mathbb{N}$  a little more systematically. In the second line there also belongs the case with  $(\tau_i, r_i) = (2, \pm 1)$ .

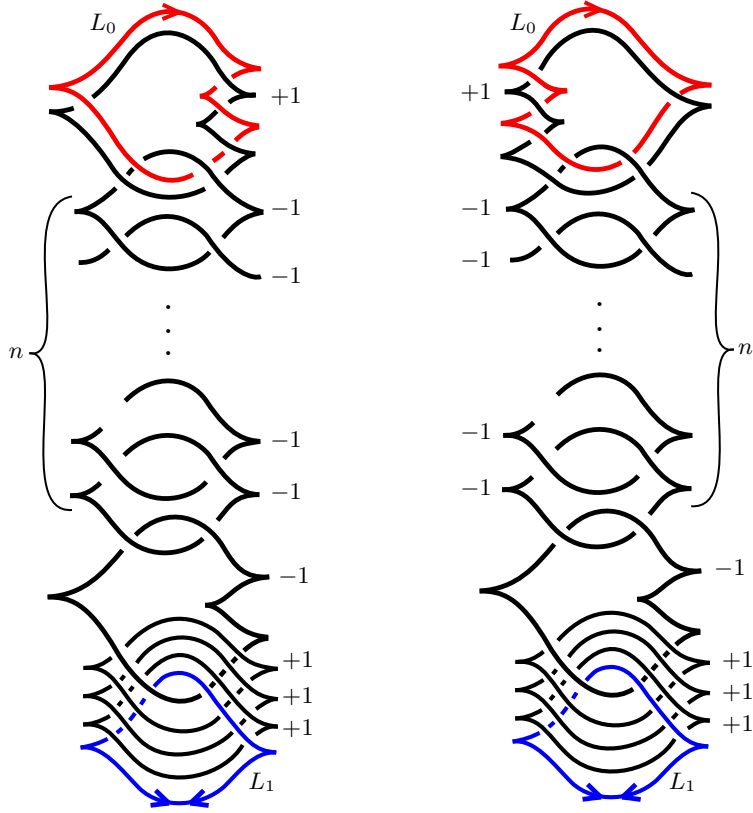


FIGURE 11. Case (c3): Legendrian Hopf links with  $\mathfrak{t}_0 \geq 4$ ,  $\mathfrak{t}_1 = 1$ .

$\mathfrak{t}_0$	$\mathfrak{r}_0$	$\mathfrak{t}_1$	$\mathfrak{r}_1$	$d_3$
$\geq 1$	$\pm(\mathfrak{t}_0 + 1)$	$\geq 1$	$\pm(\mathfrak{t}_1 + 1)$	$-1/2$
$\geq 3$	$\pm(\mathfrak{t}_0 - 3)$	$\geq 1$	$\mp(\mathfrak{t}_1 - 1)$	$3/2$
$\geq 3$	$\pm(\mathfrak{t}_0 - 1)$	$\geq 2$	$\mp(\mathfrak{t}_1 - 3)$	$3/2$
$\geq 3$	$\pm(\mathfrak{t}_0 - 1)$	$\geq 3$	$\pm(\mathfrak{t}_1 - 1)$	$3/2$

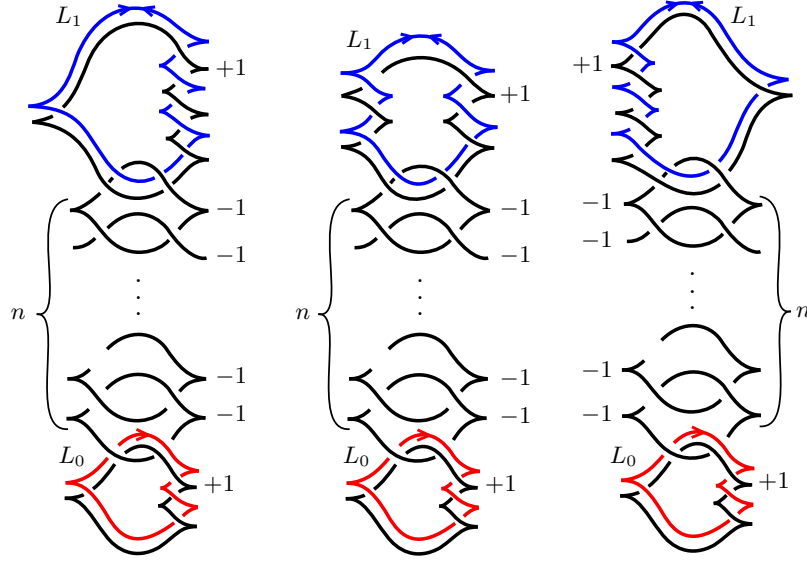
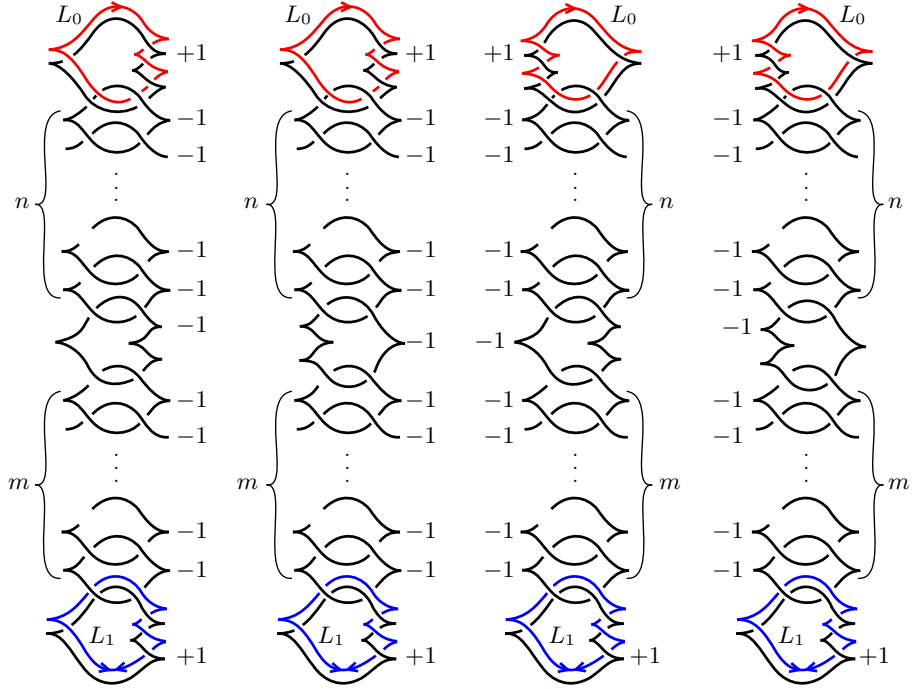
TABLE 1. Strongly exceptional realisations with  $\mathfrak{t}_0, \mathfrak{t}_1 \in \mathbb{N}$ .

### 6. CONTACT STRUCTURES ON $S^3$ AS CONTACT CUTS

In order to classify Legendrian Hopf links in  $S^3$  where the contact structure on the complement has non-zero twisting, it is useful to describe certain contact structures on  $S^3$  as contact cuts in the sense of Lerman [26]. This construction (without a reference to Lerman) was used in [8] to describe Legendrian knots and links in  $S^3$ ; see also [28, Section 2.5]. We provide additional details and simplify the computation of the classical invariants in these models of  $S^3$ .

On  $T^2 \times [0, 1]$  with coordinates  $x, y \in \mathbb{R}/\mathbb{Z}$  and  $z \in [0, 1]$  we consider the contact forms

$$(10) \quad \alpha_p = \sin\left(\frac{2p+1}{2}\pi z\right) dx + \cos\left(\frac{2p+1}{2}\pi z\right) dy, \quad p \in \mathbb{N}_0.$$

FIGURE 12. Case (c3): Legendrian Hopf links with  $\mathfrak{t}_0 \geq 3$ ,  $\mathfrak{t}_1 = 2$ .FIGURE 13. Case (c4): Legendrian Hopf links with  $\mathfrak{t}_0 \geq \mathfrak{t}_1 \geq 3$ .

These contact forms are invariant under the  $S^1$ -actions generated by  $\partial_x$  and  $\partial_y$ . Along  $\{z = 0\}$ , the vector field  $\partial_x$  is contained in  $\ker \alpha_p$ ; along  $\{z = 1\}$ , we have  $\partial_y \in \ker \alpha_p$ . By the contact cut construction [26, Proposition 2.15], the 1-form  $\alpha_p$

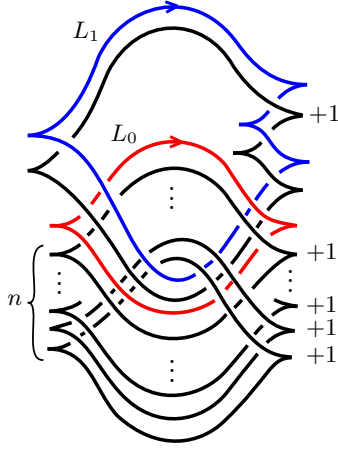


FIGURE 14. Case (d): Legendrian Hopf links with  $\tau_0 = 0$ ,  $\tau_1 \leq 0$ .

descends to a contact form on the quotient manifold obtained by collapsing the first  $S^1$ -factor in  $S^1 \times S^1 \times \{0\}$ , and the second factor in  $S^1 \times S^1 \times \{1\}$ . This quotient manifold  $T^2 \times [0, 1]/\sim$  is easily seen to be  $S^3$ , since collapsing the circles in question is topologically equivalent to attaching a copy of a solid torus  $S^1 \times D^2$  to each boundary component of  $T^2 \times [0, 1]$ , where the meridian  $\{*\} \times \partial D^2$  is sent to the first or the second  $S^1$ -factor of  $T^2$ , respectively.

Our aim in this section is to prove the following proposition. Recall that  $\xi_d$  denotes the overtwisted contact structure on  $S^3$  with  $d_3(\xi_d) = d$ .

**Proposition 6.1.** *The contact structure on  $S^3 = T^2 \times [0, 1]/\sim$  induced by the contact form  $\alpha_p$  equals*

- (i)  $\xi_{st}$  for  $p = 0$ ;
- (ii)  $\xi_{1/2}$  for  $p$  odd;
- (iii)  $\xi_{-1/2}$  for  $p \geq 2$  even.

Parts of the argument for proving this statement are contained in Examples 2.16, 2.19 and the proof of Theorem 3.1 in [26].

**Remark 6.2.** On  $T^2 \times [0, 1]$ , the contact structures  $\ker \alpha_p$  are tight, since they embed into the standard tight contact structure on  $\mathbb{R}^3$ , cf. [15, Corollary 6.5.10].

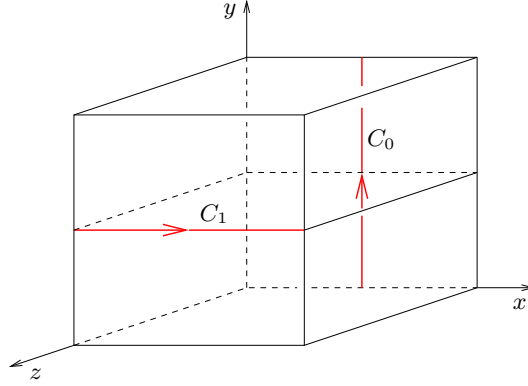
**6.1. A transverse Hopf link.** We begin with a topological preparation. The circles

$$C_0 := \left\{ \frac{1}{2} \right\} \times S^1 \times \{0\}$$

and

$$C_1 := S^1 \times \left\{ \frac{1}{2} \right\} \times \{1\}$$

in  $T^2 \times [0, 1]$  descend to unknots in  $S^3 = T^2 \times [0, 1]/\sim$ , which we continue to denote by  $C_0, C_1$ . See Figure 15, where  $T^2$  is illustrated as  $(\mathbb{R}/\mathbb{Z})^2$ . On the back face of the cube  $[0, 1]^3$  the horizontal segments are collapsed; on the front face, the vertical ones.

FIGURE 15. A transverse Hopf link in  $(S^3, \ker \alpha_p)$ .

**Lemma 6.3.** *The unknots  $C_0, C_1$  form a positive Hopf link in  $S^3$ . The unknot  $C_0$  is positively transverse to the contact structure  $\ker \alpha_p$  on  $S^3$ ; the unknot  $C_1$  is positively or negatively transverse to  $\ker \alpha_p$ , depending on  $p$  being even or odd.*

*Proof.* The horizontal square  $[0, 1] \times \{\frac{1}{2}\} \times [0, 1]$  in Figure 15 descends to a 2-disc in  $S^3$  with boundary  $C_1$ , and the unknot  $C_0$  intersects this disc positively in a single point. The transversality property of  $C_0, C_1$  is obvious from the definition of  $\alpha_p$ .  $\square$

**6.2. The standard contact structure.** Consider the 8-dimensional manifold

$$W = T^2 \times \mathbb{C} \times \mathbb{C}^2$$

with  $S^1$ -valued coordinates  $q_1, q_2$  on  $T^2 = (\mathbb{R}/2\pi\mathbb{Z})^2$ , Cartesian coordinates  $p_1 + ip_2$  on  $\mathbb{C} \setminus \{0\}$ , and polar coordinates  $(r_i, \varphi_i)$  on the last two  $\mathbb{C}$ -factors. Define a 1-form

$$\lambda = p_1 dq_1 + p_2 dq_2 + \frac{1}{2}r_1^2 d\varphi_1 + r_2^2 d\varphi_2$$

on  $W$ . Notice that the first two summands of  $\alpha$  define the canonical Liouville 1-form on  $T^2 \times \mathbb{C}$ , regarded as the unit cotangent bundle of  $T^2$ . The 2-form  $\omega = d\lambda$  is a symplectic form on  $W$ .

The vector field

$$Y = p_1 \partial_{p_1} + p_2 \partial_{p_2} + \frac{1}{2}r_1 \partial_{r_1} + \frac{1}{2}r_2 \partial_{r_2}$$

is a Liouville vector field for  $\omega$ , i.e.  $L_Y \omega = \omega$ . The vector fields

$$X_i = \partial_{q_i} - \partial_{\varphi_i}, \quad i = 1, 2,$$

are Hamiltonian vector fields for  $\omega$ , corresponding to the Hamiltonian functions  $p_i - r_i^2/2$ ,  $i = 1, 2$ . The three vector fields  $X_1, X_2, Y$  commute pairwise with each other.

The Hamiltonian  $T^2$ -action generated by  $(X_1, X_2)$  has the momentum map

$$\mu(q_1, q_2, p_1, p_2, r_1, \varphi_1, r_2, \varphi_2) = \left( p_1 - \frac{1}{2}r_1^2, p_2 - \frac{1}{2}r_2^2 \right).$$

The level set  $\mu^{-1}(0, 0)$  is regular, hence a 6-dimensional manifold, and the induced  $T^2$ -action on this manifold is free. A transversal to the  $T^2$ -action on  $\mu^{-1}(0, 0)$  is

defined by

$$\{q_1 = \varphi_1, q_2 = \varphi_2\} \subset \mu^{-1}(0, 0).$$

This shows that the reduced manifold  $\mu^{-1}(0, 0)/T^2$  is the symplectic manifold

$$(\mathbb{C}^2, r_1 dr_1 \wedge d\varphi_1 + r_2 dr_2 \wedge d\varphi_2).$$

The Liouville vector field  $Y$  is tangent to the level set  $\mu^{-1}(0, 0)$  and descends as a Liouville vector field  $\bar{Y}$  to the symplectic quotient  $\mathbb{C}^2$ . On the hypersurface

$$\left\{ \frac{1}{4}(r_1^4 + r_2^4) = 1 \right\} \subset \mathbb{C}^2,$$

which is a diffeomorphic copy of  $S^3$  transverse to  $\bar{Y}$ , this Liouville vector field induces a contact form defining  $\xi_{\text{st}}$ .

The  $\mathbb{C}$ -component  $-\partial_{\varphi_i}$  of  $X_i$  defines a free  $S^1$ -action, except at the origin  $r_i = 0$ . It follows that one equally obtains the contact structure  $\xi_{\text{st}}$  on  $S^3$  from the contact manifold

$$\{p_1^2 + p_2^2 = 1, p_1, p_2 \geq 0\} \subset T^2 \times \mathbb{C},$$

with contact form  $p_1 dq_1 + p_2 dq_2$ , by taking the quotient of the boundary components  $\{p_1 = 0\}$ ,  $\{p_2 = 0\}$  under the  $S^1$ -action defined by  $\partial_{q_1}$  and  $\partial_{q_2}$ , respectively. This is exactly the description of the contact structure on  $S^3$  as a quotient of  $(T^2 \times [0, 1], \alpha_0)$  given before Proposition 6.1, and hence proves part (i) of that proposition.

**6.3. A global frame.** In order to determine the contact structures  $\ker \alpha_p$  on  $S^3$  for  $p \geq 1$ , and for computing the classical invariants of Legendrian and transverse knots in these contact structures, we now exhibit a global frame for the contact planes  $\ker \alpha_p$  on  $S^3$ .

A global frame for  $\ker \alpha_p$  on  $T^2 \times [0, 1]$  is given by

$$(11) \quad \partial_z \quad \text{and} \quad X_p := \cos\left(\frac{2p+1}{2}\pi z\right) \partial_x - \sin\left(\frac{2p+1}{2}\pi z\right) \partial_y.$$

This frame does not, however, descend to  $S^3$ . The differential of  $\alpha_p$  is

$$d\alpha_p = \frac{2p+1}{2}\pi \cos\left(\frac{2p+1}{2}\pi z\right) dz \wedge dx - \frac{2p+1}{2}\pi \sin\left(\frac{2p+1}{2}\pi z\right) dz \wedge dy,$$

so the frame  $\partial_z, X_p$  is positive for the orientation of  $\ker \alpha_p$  defined by this 2-form. Whenever we speak of a frame for  $\ker \alpha_p$ , this orientation assumption will be understood.

Remember that at  $z = 0$ , where  $X_p = \partial_x$ , we collapse the  $x$ -circles in  $T^2$ . Figure 16 shows such a circle, with the  $z$ -direction pointing to the exterior. Performing the cut is topologically the same as filling in the circle with a disc. So the frame that extends is the one that does not rotate as one goes along the circle, for instance

$$(12) \quad \cos(2\pi x) \partial_z - \sin(2\pi x) X_p \quad \text{and} \quad \sin(2\pi x) \partial_z + \cos(2\pi x) X_p.$$

At  $z = 1$  we collapse the  $y$ -circles. Here  $X_p$  equals  $-\partial_y$  or  $\partial_y$ , depending on  $p$  being even or odd. Arguing as above, while observing that  $\partial_z$  now points into the 2-disc over which we want to extend the frame, we find that we may work with the frame

$$(13) \quad \cos(2\pi y) \partial_z - (-1)^p \sin(2\pi y) X_p \quad \text{and} \quad (-1)^p \sin(2\pi y) \partial_z + \cos(2\pi y) X_p.$$

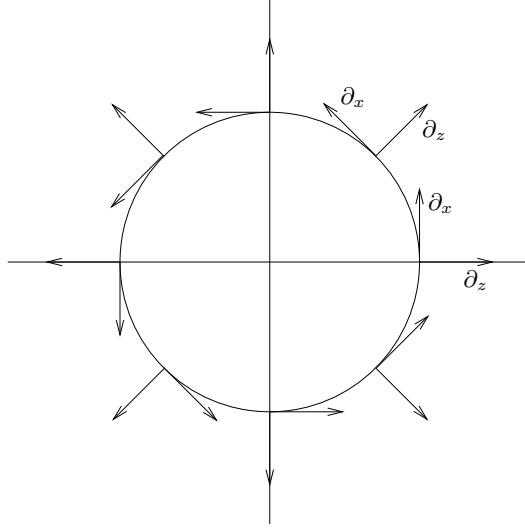


FIGURE 16. Finding the frame that descends to the cut manifold.

The extendability of the frames (12) and (13) is not affected if we rotate the first one along the  $y$ -direction, or the second one along the  $x$ -direction. This proves the following lemma.

**Lemma 6.4.** *A global positive frame for the contact structure  $\ker \alpha_p$  on  $S^3$  is given by*

$$X_p^1 := \cos(2\pi(x + (-1)^p y)) \partial_z - \sin(2\pi(x + (-1)^p y)) X_p$$

and

$$X_p^2 := \sin(2\pi(x + (-1)^p y)) \partial_z + \cos(2\pi(x + (-1)^p y)) X_p,$$

where  $X_p$  is defined in (11).  $\square$

**6.4. The  $d_3$ -invariant of  $\ker \alpha_p$ .** There are two ways to compute  $d_3(\ker \alpha_p)$ . One can directly compute the Hopf invariant of  $\ker \alpha_p$ , or one can interpret  $\ker \alpha_p$  as the contact structure obtained via a suitable  $\pi$ -Lutz twist from  $\ker \alpha_{p-1}$ .

For the first approach, we observe that the Reeb vector field of  $\alpha_p$  on  $T^2 \times [0, 1]$  is

$$R_p = \sin\left(\frac{2p+1}{2}\pi z\right) \partial_x + \cos\left(\frac{2p+1}{2}\pi z\right) \partial_y.$$

This vector field descends as the Reeb vector field of the contact form on  $S^3$  obtained via the cut construction.

As in Section 2 we normalise the Hopf invariant  $h$  such that  $h(\ker \alpha_0) = h(\xi_{st}) = 0$ , in other words, we compute the Hopf invariant of the Gauß map of a tangent 2-plane field with respect to the trivialisation of the tangent bundle  $TS^3$  defined by  $R_0, X_0^1, X_0^2$ .

The Gauß map of  $\ker \alpha_p$  is the map  $S^3 \rightarrow S^2$  given by expressing  $R_p$  in terms of the frame  $R_0, X_0^1, X_0^2$ . A straightforward computation yields

$$(14) \quad R_p = \cos(p\pi z)R_0 + \sin(p\pi z)\left(\cos(2\pi(x+y))X_0^2 - \sin(2\pi(x+y))X_0^1\right).$$



The preimage  $R_1^{-1}(s)$  of a regular value  $s \in S^2$  is a collection of circles, oriented in such a way that the transverse orientation coincides with the orientation of  $S^2$ .

**Lemma 6.5.** *The values  $\pm X_2^0 \in S^2$  are regular for the map  $R_1: S^3 \rightarrow S^2$ . The preimage  $R_1^{-1}(X_2^0)$  is the oriented circle*

$$\gamma_+: t \mapsto (x, y, z) = \left(1 - t, t, \frac{1}{2}\right);$$

the preimage  $R_1^{-1}(-X_2^0)$  equals

$$\gamma_-: t \mapsto (x, y, z) = \left(\frac{1}{2} - t, t, \frac{1}{2}\right).$$

*Proof.* From (14) it is clear that the preimages  $R_1^{-1}(\pm X_2^0)$ , as sets, are the described circles. To find the orientation of these circles, one considers the behaviour of  $R_1$  along a small meridional circle of  $\gamma_{\pm}$ . For  $\gamma_+$ , at a point on this meridional circle where  $z < 1/2$ , the vector field  $R_1$  has a positive  $R_0$ -component; for  $z > 1/2$  a negative one. For  $z = 1/2$  and  $x + y$  a little larger (resp. smaller) than 1, the vector field  $R_1$  has a negative (resp. positive)  $X_0^1$ -component. Since the transverse orientation at  $X_2^0 \in S^2$  is given by the oriented frame  $R_0, X_0^1$ , this gives the claimed orientation of  $\gamma_+$ . For  $\gamma_-$  the argument is analogous.  $\square$

*First proof of Proposition 6.1.* By pushing  $\gamma_-$  to  $z = 0$  and  $\gamma_+$  to  $z = 1$ , we see that the oriented link  $\gamma_- \sqcup \gamma_+$  is isotopic to  $C_0 \sqcup -C_1$ , hence

$$h(\ker \alpha_1) = \mathbf{lk}(\gamma_-, \gamma_+) = \mathbf{lk}(C_0, -C_1) = -1.$$

For the  $\alpha_p$  with  $p > 1$  one can argue similarly, but see also the alternative proof below.  $\square$

For the second proof of Proposition 6.1 we compute the self-linking number of the transverse unknots  $C_0, C_1$ .

**Lemma 6.6.** *The self-linking number of the transverse unknot  $C_i$ ,  $i = 0, 1$ , in  $(S^3, \ker \alpha_p)$  is  $\mathbf{sl}_{\ker \alpha_p}(C_i) = (-1)^{p+1}$ .*

*Proof.* The self-linking number  $\mathbf{sl}(K)$  of a homologically trivial transverse knot  $K$  is computed as the linking number  $\mathbf{lk}(K, K')$  with a push-off  $K'$  in the direction of a non-vanishing section of the contact structure (over a Seifert surface of  $K$  if the contact structure is not globally trivial as a 2-plane bundle).

Along  $C_0$  in  $T^2 \times [0, 1]$  we have

$$X_p^1 = \cos(\pi + (-1)^p 2\pi y) \partial_z - \sin(\pi + (-1)^p 2\pi y) \partial_x.$$

From this one finds the claimed self-linking number as the intersection number of the push-off  $C'_0$  with the disc  $\{1/2\} \times [0, 1] \times [0, 1] / \sim$ . One may push  $C_0$  a little into the  $z$ -direction if one worries about  $C_0$  sitting in the boundary of  $T^2 \times [0, 1]$  that is being partially collapsed.

Along  $C_1$  we have

$$X_p^1 = \cos((-1)^p 2\pi x + \pi) \partial_z + \sin((-1)^p 2\pi x + \pi) \partial_y,$$

and one then computes similarly.  $\square$

*Second proof of Proposition 6.1.* We already know that  $\ker \alpha_0 = \xi_{\text{st}}$ , with Hopf invariant  $h(\ker \alpha_0) = 0$ . The contact structure  $\ker \alpha_{p+1}$  on  $S^3$  is obtained from  $\ker \alpha_p$  by a  $\pi$ -Lutz twist along  $C_1$ . As in the proof of Lemma 2.2 this yields

$$h(\ker \alpha_{p+1}) = h(\ker \alpha_p) + \mathfrak{sl}_{\ker \alpha_p}(C_1) = h(\ker \alpha_p) + (-1)^p.$$

With Lemma 6.6 we find  $h(\ker \alpha_p) = 0$  for  $p$  even, and  $h(\ker \alpha_p) = -1$  for  $p$  odd. Proposition 6.1 now follows with Lemma 2.2.  $\square$

## 7. HOPF LINKS WITH TWISTING COMPLEMENT

We now describe Legendrian Hopf links in  $S^3$  equipped with one of the contact structures  $\ker \alpha_p$  from Section 6. As we shall see, any Hopf link whose complement has positive twisting can be accounted for in this way.

**7.1. Examples of torus knots.** Recall the definition of the contact form  $\alpha_p$  on  $T^2 \times [0, 1]$  given in (10). On the torus  $T^2 \times \{z\}$  this induces a non-singular linear characteristic foliation  $(T^2 \times \{z\})_{\ker \alpha_p}$  of slope  $-\tan((2p+1)\pi z/2)$ . We choose  $z \in [0, 1]$  such that this slope is a rational number  $b/a$  (including  $\infty$ ), with  $a, b$  coprime. We then have two Legendrian knots

$$\beta_{\pm}^{a,b}: t \mapsto (\pm at, \pm bt, z), \quad t \in [0, 1],$$

differing only in orientation. Regarded as knots in  $S^3$ , these are  $(a, b)$ -torus knots.

**Lemma 7.1.** *The classical invariants of  $\beta_{\pm}^{a,b}$  in  $(S^3, \ker \alpha_p)$  are  $\mathfrak{tb}(\beta_{\pm}^{a,b}) = ab$  and  $\mathfrak{rot}(\beta_{\pm}^{a,b}) = \pm(a + (-1)^p b)$ .*

*Proof.* As a push-off of  $\beta_{\pm}^{a,b}$  in a direction transverse to  $\ker \alpha_p$  we can simply take a parallel copy on  $T^2 \times \{z\}$ . The Thurston–Bennequin invariant is the linking number of  $\beta_{\pm}^{a,b}$  with this push-off, which equals  $ab$ .

For the rotation number of  $\beta_{+}^{a,b}$  we need to count the number of rotations of  $X_p$  (which is tangent to  $\beta_{+}^{a,b}$ ) relative to the frame  $X_p^1, X_p^2$  as we traverse  $\beta_{+}^{a,b}$  once in positive direction. Equivalently, we need to count negatively the number of rotations of  $X_p^1$  relative to the frame  $\partial_z, X_p$ . Along  $\beta_{+}^{a,b}$  we have, with Lemma 6.4,

$$X_p^1(\beta_{+}^{a,b}(t)) = \cos(2\pi(a + (-1)^p b)t) \partial_z - \sin(2\pi(a + (-1)^p b)t) X_p(\beta_{+}^{a,b}(t)).$$

This yields the claimed result  $\mathfrak{rot}(\beta_{\pm}^{a,b}) = \pm(a + (-1)^p b)$ .  $\square$

These examples were first described by Dymara [8], who computed their classical invariants from a generalised front projection.

**7.2. Examples of Hopf links.** Given  $p \in \mathbb{N}_0$  and  $a \in \mathbb{Z}$ , let  $z_a \in (0, \frac{2}{2p+1})$  be the unique number such that

$$-\tan\left(\frac{2p+1}{2}\pi z_a\right) = \frac{1}{a}.$$

If  $p = 0$  we assume in addition that  $a < 0$ , so that  $z_a \in (0, 1)$  in this case, too. The Legendrian knot  $\beta_0 := \beta_{+}^{a,1}$ , corresponding to this choice of  $z$ , i.e.  $\beta_0(t) = (at, t, z_a)$ , is isotopic to  $C_0$ .

Observe that the slope of the characteristic foliation  $(T^2 \times \{z\})_{\ker \alpha_p}$  decreases monotonically from 0 to  $-\infty$  and then from  $\infty$  to 0 as  $z$  goes from 0 to  $\frac{2}{2p+1}$ . Hence, any parallel copy  $\beta_{0,z}: t \mapsto (at, t, z)$  of  $\beta_0$  with  $0 < z < z_a$  is positively transverse

to  $\ker \alpha_p$ , see Figure 17. For  $z = 0$ , this curve coincides with  $C_0$  in  $S^3$ . This means that any such parallel curve constitutes the positive transverse push-off of  $\beta_0$  and is transversely isotopic to  $C_0$ .

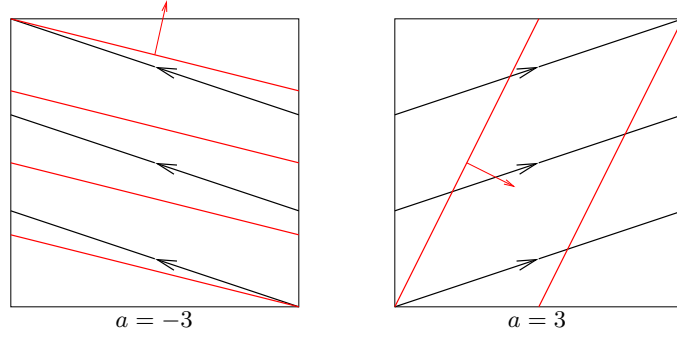


FIGURE 17.  $\beta_{0,z}$  is positively transverse to  $\ker \alpha_p$  for  $z < z_a$ .

In a completely analogous fashion, given  $b \in \mathbb{Z}$ , let  $z_b \in (1 - \frac{2}{2p+1}, 1)$  be the unique number such that

$$-\tan\left(\frac{2p+1}{2}\pi z_b\right) = b.$$

Again, for  $p = 0$  we have to assume  $b < 0$ . The Legendrian knot  $\beta_1 := \beta_+^{1,b}$  is isotopic to  $C_1$ . Any parallel copy  $t \mapsto (t, bt, z)$  with  $z_b < z < 1$  is positively resp. negatively transverse to  $\ker \alpha_p$ , depending on  $p$  being even or odd, and transversely isotopic to  $C_1$ .

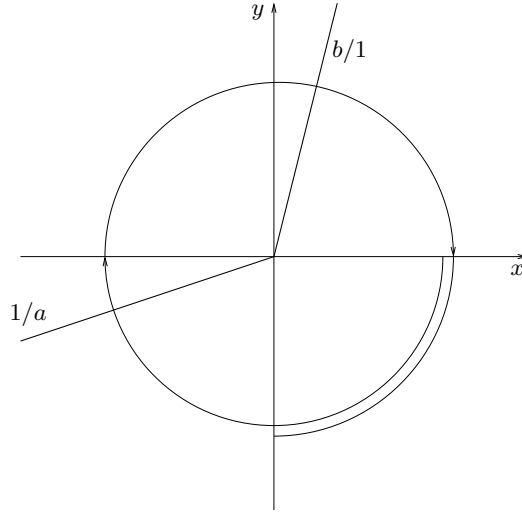


FIGURE 18. Realising  $\beta_0 \sqcup \beta_1$  as a Legendrian Hopf link in  $\ker \alpha_p$ .

When  $z_a < z_b$ , the link  $\beta_0 \sqcup \beta_1$  constitutes a positive Hopf link in  $(S^3, \ker \alpha_p)$ . Figure 18 illustrates that for  $a, b > 0$  we need to have  $p \geq 2$  to achieve  $z_a < z_b$ . For  $a, b < 0$  we can take any  $p \in \mathbb{N}_0$ . In all other cases, any  $p \geq 1$  will do.

**Proposition 7.2.** *The Hopf link  $\beta_0 \sqcup \beta_1$  in  $(S^3, \ker \alpha_p)$  is exceptional.*

*Proof.* Suppose there were an overtwisted disc in  $S^3 \setminus (\beta_0 \sqcup \beta_1)$ . This disc would persist in the complement of the transverse push-off  $\beta_0^T \sqcup \beta_1^T$  of  $\beta_0 \sqcup \beta_1$ , since  $\beta_0^T \sqcup \beta_1^T$  can be chosen as close to  $\beta_0 \sqcup \beta_1$  as we like. But  $\beta_0^T \sqcup \beta_1^T$  is transversely and hence, by [15, Theorem 2.6.12], ambiently contact isotopic to  $C_0 \sqcup C_1$ , whose complement is tight by Remark 6.2.  $\square$

The case  $a = b = 0$  of this result was proved by Dymara [8, Proposition 4.9], using a more complicated argument. Dymara also showed that  $\beta_{\pm}^{a,b}$  in  $(S^3, \ker \alpha_1) = (S^3, \xi_{1/2})$  is exceptional for  $ab > 0$ . We can give a very simple proof of this fact, similar to the one above, if one of  $a, b$  equals 1.

**Proposition 7.3.** *The unknots  $\beta_{\pm}^{a,1}$  and  $\beta_{\pm}^{1,b}$  with  $a, b > 0$  in  $(S^3, \ker \alpha_1)$  are exceptional.*

*Proof.* As illustrated in [28, Figure 6], an  $(a-1)$ -fold negative stabilisation of  $\beta_{+}^{a,1}$  yields  $\beta_{+}^{1,1}$ ; the other cases are analogous.

Suppose  $\beta_{+}^{a,1}$  were loose. Then so would be its stabilisation  $\beta := \beta_{+}^{1,1}$ . The overtwisted disc would persist in the complement of two parallel copies  $\beta_{z_0}, \beta_{z_1}$  of  $\beta_{+}^{1,1}$ , with  $z_0 < \frac{1}{2} < z_1$  close to  $\frac{1}{2}$ . But the link  $\beta_{z_0} \sqcup \beta_{z_1}$  is transverse to  $\ker \alpha_1$ , and transversely isotopic to  $C_0 \sqcup C_1$ , whose complement is tight.  $\square$

**7.3. Computing the twisting.** We now want to show that if we take the minimal  $p$  in the above construction, i.e.  $p \in \{0, 1, 2\}$  depending on the values of  $a$  and  $b$ , the complement of  $\beta_0 \sqcup \beta_1$  in  $(S^3, \ker \alpha_p)$  will be minimally twisting. We consider the case  $a, b > 0$  and  $p = 2$  illustrated in Figure 18. The other cases are analogous.

First of all, we observe that we have a canonical identification of  $S^3 \setminus (\beta_0 \sqcup \beta_1)$  with  $T^2 \times (0, 1)$  as in Section 3, given by identifying the first  $S^1$ -factor of  $T^2$  with a meridian of  $\beta_0$ , and the second  $S^1$ -factor with a meridian of  $\beta_1$ . This gives us a well-defined notion of twisting of a contact structure on this link complement as a positive real number, not just an integer, cf. the discussion in [24, Section 2.2.1].

The thickened torus  $T^2 \times [z_a + \varepsilon, z_b - \varepsilon]$ , where  $\varepsilon > 0$  is chosen sufficiently small, lies in the complement of  $\beta_0 \sqcup \beta_1$ . The twisting of  $\ker \alpha_p$  on this thickened torus is greater than  $\pi/2$ , but smaller than  $\pi$ . (In particular, it is minimally twisting in the sense of [24].)

Arguing by contradiction, we assume that  $(S^3 \setminus (\beta_0 \sqcup \beta_1), \ker \alpha_2)$  is not minimally twisting. Under the canonical identification of the complement of a small open tubular neighbourhood of  $\beta_0 \sqcup \beta_1$  with  $T^2 \times [0, 1]$ , the boundary slope is close to  $1/a$  at  $z = 0$  and close to  $b/1$  at  $z = 1$ . Hence, if  $T^2 \times [0, 1]$  is not minimally twisting, it will have twisting larger than  $3\pi/2$ . Indeed, we find two embedded convex tori (in the isotopy class of  $T^2 \times \{*\}$ ) of slope 0 and slope  $-\infty$ , respectively, bounding a thickened torus of twisting  $3\pi/2$ , see [24, Corollary 4.8] and cf. Figure 18.

Again, this thickened torus of twisting  $3\pi/2$  would persist in the complement of a tubular neighbourhood of  $C_0 \sqcup C_1$ . In the tubular neighbourhood of  $C_0$  we find a convex torus with slope  $-1/n$  for  $n \in \mathbb{N}$  sufficiently large, in the same isotopy class as the other 2-tori we are considering in  $S^3 \setminus (C_0 \sqcup C_1)$ . Similarly, near  $C_1$  we find such a convex torus with slope  $-m$  for  $m \in \mathbb{N}$  sufficiently large. So the slope would have to decrease from  $-1/n$  to 0 via  $-\infty$  and then, after twisting by  $3\pi/2$ , from  $\infty$  to  $-m$ . This would add up to a twisting of more than  $5\pi/2$ , which is impossible.

**7.4. Proof of Theorem 1.2 (e).** We now provide details of the exceptional Legendrian Hopf links where the contact structure on the link complement has positive twisting. All claims follow from the preceding discussion. Together with Proposition 3.2, which gives an upper bound on the number of such realisations, this constitutes a proof of Theorem 1.2 (e). The following three cases cover all eventualities, possibly after exchanging the roles of  $L_0$  and  $L_1$ .

7.4.1.  $\mathfrak{t}_0, \mathfrak{t}_1 > 0$ . Here the  $\pi$ -twisting in the complement equals  $p - 2$ . For  $p \geq 2$  even, we have the two realisations with  $(\mathfrak{tb}, \mathfrak{rot})$  equal to

$$(\mathfrak{t}_0, \pm(\mathfrak{t}_0 + 1)) \quad \text{and} \quad (\mathfrak{t}_1, \pm(\mathfrak{t}_1 + 1)) \quad \text{in } \xi_{-1/2}.$$

For  $p \geq 3$  odd, we can realise

$$(\mathfrak{t}_0, \pm(\mathfrak{t}_0 - 1)) \quad \text{and} \quad (\mathfrak{t}_1, \mp(\mathfrak{t}_1 - 1)) \quad \text{in } \xi_{1/2}.$$

For  $\mathfrak{t}_0 = \mathfrak{t}_1 = 1$ , this is only a single realisation. From Figure 18 one sees that each individual component  $\beta_0, \beta_1$  is loose, since the contact planes twist by more than  $\pi$  in its complement. For instance, in the complement of  $\beta_1$  in  $(S^3, \ker \alpha_2)$  we have the overtwisted disc

$$\left\{ x \in [0, 1], y = \frac{1}{2}, 0 \leq z \leq \frac{2}{5} \right\} / \sim.$$

The case  $p = 2$  coincides with the corresponding subcases in the classification of strongly exceptional Hopf links.

7.4.2.  $\mathfrak{t}_0, \mathfrak{t}_1 < 0$ . The invariants in this and the third case below are the same as in the first case. The only difference is that here the  $\pi$ -twisting in the complement equals  $p$ , and one may consider any  $p \geq 0$ . For  $p = 0$ , one obtains a realisation in the tight  $\xi_{\text{st}}$ ; for  $p \geq 1$  the two link components are loose. For  $p \geq 0$  even and  $\mathfrak{t}_0 = \mathfrak{t}_1 = -1$ , there is only one realisation.

7.4.3.  $\mathfrak{t}_0 \leq 0, \mathfrak{t}_1 \geq 0$ . Here the twisting is  $p - 1$ , and one may consider any  $p \geq 1$ . The components  $\beta_0, \beta_1$  are loose, except for the unknot  $\beta_1$  in the case  $p = 1$  and  $\mathfrak{t}_1 \geq 1$ , which is exceptional by [8, Proposition 5.5]. (Beware that Dymara's notational conventions differ from ours.)

The latter case coincides with the corresponding examples in Section 5, as one can see by looking at the invariants in Table 2. For  $\mathfrak{t}_0 = 0$  we are in case (d). For  $\mathfrak{t}_0 < 0$  and  $\mathfrak{t}_1 = 0$  we are in case (d) with the roles of  $L_0$  and  $L_1$  exchanged. For  $\mathfrak{t}_0 < 0$  and  $\mathfrak{t}_1 = 1$  we obtain examples from case (b2). For  $\mathfrak{t}_0 < 0$  and  $\mathfrak{t}_1 \geq 2$ , one finds the same examples in case (b1): when  $n$  is even, take  $k = -\mathfrak{t}_0$  and  $\ell = 0$ ; when  $n$  is odd, choose  $\ell = -\mathfrak{t}_0$  and  $k = 0$ .

## 8. LOOSE HOPF LINKS

In this section we prove part (f) of Theorem 1.2. As shown in [12], the classification of loose Legendrian knots in any contact 3-manifold reduces to a homotopical question, see also [16]. However, rather than relying on this general theory, which would have to be adapted to links, we shall give an *ad hoc* proof that relies on the topology of the link complement in our situation.

**8.1. Finding a Legendrian realisation.** We begin by showing that in any given overtwisted  $(S^3, \xi_d)$  one can find a loose Legendrian Hopf link realising any combination of values  $(\mathfrak{t}_0, \mathfrak{r}_0, \mathfrak{t}_1, \mathfrak{r}_1)$  for the classical invariants, subject only to the condition that  $\mathfrak{t}_i + \mathfrak{r}_i$  be odd,  $i = 0, 1$ .

Start with any topological Hopf link in  $(S^3, \xi_d)$  with overtwisted complement. Construct a loose Legendrian Hopf link as a  $C^0$ -approximation of this topological Hopf link; such an approximation exists by [15, Theorem 3.3.1]. Also, the components of this Legendrian Hopf link will satisfy the parity condition on  $\mathfrak{tb} + \mathfrak{rot}$ , since this is a general phenomenon in contact 3-manifolds, see [15, Remark 4.6.35].

By stabilising the components of this Hopf link, one can increase or decrease the rotation number in steps of 1, while decreasing the Thurston–Bennequin invariant by 1 with each stabilisation. This is a local process and preserves the overtwisted disc in the complement. In this way, we can find a loose Legendrian realisation which has the correct values  $\mathfrak{r}_0, \mathfrak{r}_1$  of rotation numbers.

We can always decrease the value of  $\mathfrak{tb}$  of a Legendrian knot in steps of 2, while keeping  $\mathfrak{rot}$  unchanged, by adding further pairs of positive and negative stabilisations.

In an overtwisted contact 3-manifold one can find a loose Legendrian unknot  $K_{1,0}$  with  $\mathfrak{tb}(K_{1,0}) = 1$  and  $\mathfrak{rot}(K_{1,0}) = 0$ , by forming the connected sum of two Legendrian knots bounding an overtwisted disc (with opposite orientations), see [15, p. 317].

The connected sum of a Legendrian knot  $L$  with  $K_{1,0}$  can be performed in such a way that the topological knot type and  $\mathfrak{rot}(L)$  remain unchanged, and such that  $\mathfrak{tb}(L)$  increases by 2; again, see [15, p. 317]. In this way, we can adjust our Legendrian Hopf link so that it also has the correct values  $\mathfrak{t}_0, \mathfrak{t}_1$  of Thurston–Bennequin invariants (and remains loose).

**8.2. Uniqueness of the Legendrian realisation.** Let  $L_0 \sqcup L_1$  and  $L'_0 \sqcup L'_1$  be two loose Legendrian realisations of the Hopf link in some overtwisted  $(S^3, \xi_d)$  with  $\mathfrak{tb}(L_i) = \mathfrak{tb}(L'_i)$  and  $\mathfrak{rot}(L_i) = \mathfrak{rot}(L'_i)$ ,  $i = 0, 1$ .

The Thurston–Bennequin invariant measures the twisting of the contact framing relative to the surface framing. These invariants being equal for  $L_i$  and  $L'_i$  implies, by the proof of the Legendrian neighbourhood theorem [15, Theorem 2.5.8], that we can find a topological diffeotopy  $\phi_t$  of  $S^3$  starting at  $\phi_0 = \text{id}_{S^3}$  and ending at a diffeomorphism  $\phi_1$  of  $S^3$  that sends an open tubular neighbourhood  $U$  of  $L_0 \sqcup L_1$  *contactomorphically* to a neighbourhood of  $L'_0 \sqcup L'_1$ .

We need to show that the contact structures  $\xi_d$  and  $\phi_{1*}^{-1}\xi_d$  on  $S^3 \setminus U \cong T^2 \times [0, 1]$  are diffeomorphic rel boundary (perhaps for a slightly ‘thinner’  $U$ ). By Eliashberg’s classification [9] of overtwisted contact structures, see also [15, Section 4.7] and the work of Borman–Eliashberg–Murphy [1], it suffices to show that  $\xi_d$  and  $\phi_{1*}^{-1}\xi_d$  on  $T^2 \times [0, 1]$  are homotopic rel boundary as tangent 2-plane fields.

The identification of  $S^3 \setminus U$  with  $T^2 \times [0, 1]$  is chosen as in Sections 3 and 7.3. That is, the first  $S^1$ -factor of  $T^2$  defines a meridian of  $L_0$ , the second factor a meridian of  $L_1$ . As before, we write the coordinates on  $T^2 \times [0, 1]$  as  $x, y \in \mathbb{R}/\mathbb{Z}$  and  $z \in [0, 1]$ .

As an abstract 2-plane bundle over  $S^3$ , the contact structure  $\xi_d$  is trivial, since its Euler class is zero. This allows us to choose an orthonormal frame  $X_1, X_2, X_3$  for the tangent bundle of  $S^3$ , with respect to an auxiliary Riemannian metric, with  $X_1, X_2$  a positive frame for  $\xi_d$ , and  $X_3$  positively orthonormal to it. Likewise, we

choose such an orthonormal frame  $X'_1, X'_2, X'_3$  for  $\phi_{1*}^{-1}\xi_d$ . By writing the vectors in this second frame in terms of  $X_1, X_2, X_3$  we define a map  $\Phi: S^3 \rightarrow \text{SO}(3)$ .

We first look at a closed tubular neighbourhood  $\nu L_0$  of  $L_0$ , contained in  $U$ . This may be chosen as a standard neighbourhood with convex boundary. In particular, we find a Legendrian longitude  $L_0^\parallel$  on the boundary  $\partial(\nu L_0)$  that is Legendrian isotopic to  $L_0$ . This can easily be seen in a model

$$(S^1 \times D^2, \ker(\cos \theta dx_1 - \sin \theta dx_2))$$

for  $\nu L_0$ , where the longitude  $L_0^\parallel$  in question is defined by

$$\theta \mapsto (\cos \theta, -\sin \theta, \theta).$$

The linking number of  $L_0^\parallel$  with  $L_0$  in  $S^3$  equals  $\text{tb}(L_0)$ .

On  $\nu L_0$ , the contact structures  $\xi_d$  and  $\phi_{1*}^{-1}\xi_d$  coincide, hence so do  $X_3$  and  $X'_3$ . Along  $L_0^\parallel$  we can count the rotations  $\mathbf{r}, \mathbf{r}'$  of the tangent direction of  $L_0^\parallel$  relative to the frames  $X_1, X_2$  and  $X'_1, X'_2$ . These are the rotation numbers of  $L_0^\parallel$  (or its Legendrian isotopic copy  $L_0$ ) with respect to  $\xi_d$  and  $\phi_{1*}^{-1}\xi_d$ , respectively. From the assumption that  $\text{rot}(L_0) = \text{rot}(L'_0)$  we conclude  $\mathbf{r} = \mathbf{r}'$ . Thus, after a homotopy of  $X'_1, X'_2$  we may assume that this frame coincides with  $X_1, X_2$  along  $L_0^\parallel$ .

Both  $X_1, X_2$  and  $X'_1, X'_2$  define a frame of  $\xi_d$  over each meridional disc in  $\nu L_0$ . Therefore, their relative twisting along any meridian is zero, and after a further homotopy of  $X'_1, X'_2$  we may assume that this frame coincides with  $X_1, X_2$  over all of  $\nu L_0$ . The same argument can be applied to  $\nu L_1$ .

The map  $\Phi$  comparing the two frames  $X_1, X_2, X_3$  and  $X'_1, X'_2, X'_3$  then restricts to a map

$$\Phi: (T^2 \times [0, 1], T^2 \times \{0, 1\}) \longrightarrow (\text{SO}(3), \text{id}_{\mathbb{R}^3}).$$

**Lemma 8.1.** *Possibly after a modification of  $X'_1, X'_2$  near the boundary  $T^2 \times \{0, 1\}$  that fixes the contact structure  $\phi_{1*}^{-1}\xi_d$ , the map  $\Phi$  is homotopic rel boundary to a map that equals the constant map to  $\text{id}_{\mathbb{R}^3}$  outside an open 3-ball in  $T^2 \times [0, 1]$ .*

*Proof.* The restriction of  $\Phi$  to the path  $t \mapsto (0, 0, t)$ ,  $t \in [0, 1]$ , in  $T^2 \times [0, 1]$  defines a loop in  $\text{SO}(3)$  based at  $\text{id}_{\mathbb{R}^3}$ . Since  $\pi_1(\text{SO}(3)) = \mathbb{Z}_2$ , this may or may not be trivial. If it is not, we add a full twist to the frame  $X'_1, X'_2$  relative to  $X_1, X_2$  as we go out in radial direction in  $\nu L_0$ , and we undo this twist in  $z$ -direction in a neighbourhood of  $T^2 \times \{0\}$  inside  $T^2 \times [0, 1]$  where  $\xi_d$  and  $\phi_{1*}^{-1}\xi_d$  coincide.

After this modification (if necessary) and a homotopy of  $X'_1, X'_2, X'_3$  rel boundary, we may assume that the two frames coincide along the described path.

The restriction of  $\Phi$  to the cylinder  $\{x = 0, y \in S^1, z \in [0, 1]\}$ , sliced open along the path we just discussed, defines an element of  $\pi_2(\text{SO}(3)) = 0$ . Thus, after yet another homotopy rel boundary we may assume that  $\Phi = \text{id}_{\mathbb{R}^3}$  also on this cylinder. The same argument applies to the cylinder  $\{x \in S^1, y = 0, z \in [0, 1]\}$ .

We have now achieved that  $\Phi$  equals the constant map to  $\text{id}_{\mathbb{R}^3}$  outside the open 3-ball

$$\text{Int}(D^3) = (0, 1)^3 \subset T^2 \times [0, 1] \subset S^3.$$

In particular, this means that we have homotoped  $\phi_{1*}^{-1}\xi_d$  to a tangent 2-plane field on  $S^3$  that coincides with  $\xi_d$  outside  $\text{Int}(D^3)$ .  $\square$

Over  $S^3$ , the two tangent 2-plane fields  $\xi_d$  and  $\phi_1^{-1}\xi_d$  are homotopic, detected by their Hopf invariants being equal. This means that the obstruction to homotopy of the two tangent 2-plane fields over the closed 3-ball  $D^3$  rel  $\partial D^3$  vanishes.

## 9. SOME COMPUTATIONS

In this section we collect the computations of the classical invariants for some of the examples in Section 5.5. The surgery knots in the diagrams are ordered from top to bottom and oriented clockwise for the purpose of computing linking and rotation numbers. The results of all computations are collected in Table 2.

9.1. **Figure 9.** The linking matrix is

$$\begin{pmatrix} -2 & -1 & -1 & -1 \\ -1 & 0 & -1 & -1 \\ -1 & -1 & 0 & -1 \\ -1 & -1 & -1 & 0 \end{pmatrix}.$$

The extended linking matrices for  $L_0$  and  $L_1$  are

$$M_0 = \left( \begin{array}{c|cccc} 0 & 3 & 1 & 1 & 1 \\ \hline 3 & & & & \\ 1 & & M & & \\ 1 & & & & \\ 1 & & & & \end{array} \right) \quad \text{and} \quad M_1 = \left( \begin{array}{c|cccc} 0 & -1 & -1 & -1 & -1 \\ \hline -1 & & & & \\ -1 & & M & & \\ -1 & & & & \\ -1 & & & & \end{array} \right),$$

respectively. The determinants are

$$\det M = 1, \quad \det M_0 = 6, \quad \text{and} \quad \det M_1 = 2.$$

This gives  $\text{tb}(L_0) = 3$  and  $\text{tb}(L_1) = 1$ .

For the diagram on the left of Figure 9 we have

$$\text{rot}(L_0) = \text{rot}_0 - \left\langle \begin{pmatrix} 2 \\ 0 \\ 0 \\ 0 \end{pmatrix}, M^{-1} \begin{pmatrix} 3 \\ 1 \\ 1 \\ 1 \end{pmatrix} \right\rangle = -2 - \left\langle \begin{pmatrix} 2 \\ 0 \\ 0 \\ 0 \end{pmatrix}, \begin{pmatrix} -3 \\ 1 \\ 1 \\ 1 \end{pmatrix} \right\rangle = 4$$

and

$$\text{rot}(L_1) = \text{rot}_1 - \left\langle \begin{pmatrix} 2 \\ 0 \\ 0 \\ 0 \end{pmatrix}, M^{-1} \begin{pmatrix} -1 \\ -1 \\ -1 \\ -1 \end{pmatrix} \right\rangle = 0 - \left\langle \begin{pmatrix} 2 \\ 0 \\ 0 \\ 0 \end{pmatrix}, \begin{pmatrix} -1 \\ 1 \\ 1 \\ 1 \end{pmatrix} \right\rangle = 2.$$

For the diagram on the right of Figure 9, the vector  $\underline{\text{rot}}$  of rotation numbers is the zero vector, so the computation simplifies and yields  $\text{rot}(L_0) = \text{rot}(L_1) = 0$ .

The signature of  $M$  is zero. This can be seen from the Kirby diagram in Figure 4. Simply count how many  $(\pm 1)$ -framed unknots are left after all blow-downs, minus those introduced to replace the twisting boxes. There are four 2-handles, hence  $\chi = 5$ . For the diagram on the left, the solution  $\mathbf{x}$  of  $M\mathbf{x} = \underline{\text{rot}}$  is  $\mathbf{x} = (-4, 2, 2, 2)^t$ ; on the right,  $\mathbf{x}$  is the zero vector. This gives  $c^2 = -8$  in the first and  $c^2 = 0$  in the second case, resulting in the values of  $d_3$  listed in Table 2. The contact structure described by the surgery diagram on the left is the overtwisted structure  $\xi_{-1/2}$  (rather than  $\xi_{\text{st}}$ , which also has  $d_3 = -\frac{1}{2}$ ), since  $L_0$  and  $L_1$  violate the Bennequin inequality [15, Theorem 4.6.36] for Legendrian knots in tight contact 3-manifolds.



Case	Figure	$\mathfrak{t}_0$	$\mathfrak{r}_0$	$\mathfrak{t}_1$	$\mathfrak{r}_1$	type	$d_3$	no. of realisations
b1	7	$-(k + \ell) < 0$	$\pm(\ell - k - (-1)^n)$	$n + 2 \geq 2$	$\mp(-1)^n(n + 1)$	loose/exc.	1/2	$2 \mathfrak{t}_0 - 1 $
b2	8	$< 0$	$\mathfrak{t}_0 - 1, \mathfrak{t}_0 + 1, \dots, -\mathfrak{t}_0 - 1, -\mathfrak{t}_0 + 1$	1	0	loose/exc.	1/2	$ \mathfrak{t}_0 - 2 $
c1	8	1	0	1	0	exc./exc.	1/2	1
c2	Section 7.4.1	2	$\pm 3$	1	$\pm 2$	loose/loose	-1/2	2
	9	3	$\pm 4$	1	$\pm 2$	loose/loose	-1/2	2
		3	0	1	0	loose/loose	3/2	1
	10	2	$\pm 3$	2	$\pm 3$	loose/loose	-1/2	2
		2	$\pm 1$	2	$\pm 1$	loose/loose	3/2	2
c3	11	$\geq 4$	$\pm(\mathfrak{t}_0 + 1)$	1	$\pm 2$	loose/loose	-1/2	2
		$\geq 4$	$\pm(\mathfrak{t}_0 - 3)$	1	0	loose/loose	3/2	2
	12	$\geq 3$	$\pm(\mathfrak{t}_0 + 1)$	2	$\pm 3$	loose/loose	-1/2	2
		$\geq 3$	$\pm(\mathfrak{t}_0 - 1)$	2	$\pm 1$	loose/loose	3/2	2
		$\geq 3$	$\pm(\mathfrak{t}_0 - 3)$	2	$\mp 1$	loose/loose	3/2	2
c4	13	$\geq 3$	$\pm(\mathfrak{t}_0 + 1)$	$\geq 3$	$\pm(\mathfrak{t}_1 + 1)$	loose/loose	-1/2	2
		$\geq 3$	$\pm(\mathfrak{t}_0 - 1)$	$\geq 3$	$\pm(\mathfrak{t}_1 - 1)$	loose/loose	3/2	2
		$\geq 3$	$\pm(\mathfrak{t}_0 - 3)$	$\geq 3$	$\mp(\mathfrak{t}_1 - 1)$	loose/loose	3/2	2
		$\geq 3$	$\pm(\mathfrak{t}_0 - 1)$	$\geq 3$	$\mp(\mathfrak{t}_1 - 3)$	loose/loose	3/2	2
d	7, 8	0	$\pm 1$	$\geq 1$	$\pm(\mathfrak{t}_1 - 1)$	loose/exc.	1/2	2
	14	0	$\pm 1$	$\leq 0$	$\pm(\mathfrak{t}_1 - 1)$	loose/loose	1/2	2

TABLE 2. The complete list of strongly exceptional realisations.

The Legendrian Hopf link  $L_0 \sqcup L_1$  is exceptional, since contact  $(-1)$ -surgery along  $L_0$  and contact  $(-1)$ -surgery along  $L_1$  and two Legendrian push-offs of  $L_1$  leads, by the cancellation lemma, to the empty diagram, that is,  $(S^3, \xi_{st})$ . The individual components  $L_0, L_1$  are loose, however, since there are no exceptional unknots in  $(S^3, \xi_{-1/2})$  or  $(S^3, \xi_{3/2})$ . The same arguments apply to the examples in Figure 10.

**9.2. Figure 11.** Here we only collect the data the reader needs to verify our claim about the invariants in this case listed in Table 2. As linking matrix  $M$  we take the one given by ordering the surgery curves from top to bottom, all oriented clockwise. The signature of this matrix is  $\sigma = -n - 1$ . This can be read off from the Kirby moves as explained in the previous example. The Euler characteristic is  $\chi = n + 6$ .

Rather than computing the Thurston–Bennequin invariants of  $L_0$  and  $L_1$  from the extended linking matrices, one can simply keep control over the contact framing during the Kirby moves described in Figures 5 and 2. We find  $\text{tb}(L_0) = n + 4$  and  $\text{tb}(L_1) = 1$ .

For the figure on the left, the vector  $\mathbf{x}$  with  $M\mathbf{x} = \underline{\text{rot}}$  is

$$\mathbf{x} = (-(n+1), n, -(n-1), \dots, -1, 0, 0, 0, 0)^t \quad \text{for } n \geq 0 \text{ even}$$

and

$$\mathbf{x} = (-(n+5), n+4, -(n+3), \dots, 5, -4, 2, 2, 2)^t \quad \text{for } n \geq 1 \text{ odd.}$$

This gives  $d_3 = \frac{3}{2}$  for  $n$  even, and  $d_3 = -\frac{1}{2}$  for  $n$  odd.

For the figure on the right, we have

$$\mathbf{x} = (n+5, -(n+4), \dots, 5, -4, 2, 2, 2)^t \quad \text{for } n \text{ even}$$

and

$$\mathbf{x} = (n+1, -n, n-1, \dots, -1, 0, 0, 0, 0)^t \quad \text{for } n \text{ odd,}$$

leading to  $d_3 = -\frac{1}{2}$  for  $n$  even and  $d_3 = \frac{3}{2}$  for  $n$  odd.

For the clockwise orientation of  $L_0$  and  $L_1$  (beware that for  $n$  odd this gives a negative Hopf link) we have

$$\underline{\mathbf{k}}_0 = (-2, -1, 0, \dots, 0)^t$$

and

$$\underline{\mathbf{k}}_1 = (1, \underbrace{0, \dots, 0}_n, -1, -1, -1, -1)^t$$

for the vector of linking numbers of  $L_0$  and  $L_1$ , respectively, with the surgery curves. This yields

$$M^{-1}\underline{\mathbf{k}}_0 = (n+4, -(n+2), n+1, \dots, (-1)^n 3, (-1)^{n+1} 2, (-1)^n, (-1)^n, (-1)^n)^t$$

and

$$M^{-1}\underline{\mathbf{k}}_1 = ((-1)^n, (-1)^{n-1}, (-1)^{n-2}, \dots, -1, 1, 1, 1)^t.$$

The remaining calculations are then straightforward.

The arguments for the looseness of the components and the exceptionality of the link are as in the previous case.

9.3. **Figure 14.** The linking matrix is the  $((n + 1) \times (n + 1))$ -matrix

$$M = M^{(n)} = \begin{pmatrix} -1 & -1 & -1 & \cdots & -1 \\ -1 & 0 & -1 & \cdots & -1 \\ -1 & -1 & \ddots & \cdots & -1 \\ \vdots & \vdots & & \cdots & \vdots \\ -1 & -1 & -1 & \cdots & 0 \end{pmatrix}$$

The extended linking matrices are

$$M_0^{(n)} = \left( \begin{array}{c|ccc} 0 & -1 & \cdots & -1 \\ \hline -1 & & & \\ \vdots & & & \\ -1 & & & \end{array} \right)$$

and

$$M_1^{(n)} = \left( \begin{array}{c|ccc} 0 & -2 & -1 & \cdots & -1 \\ \hline -2 & & & & \\ -1 & & & & \\ \vdots & & & & \\ -1 & & & & \end{array} \right).$$

One easily computes  $\det M^{(n)} = -1$ ,  $\det M_0^{(n)} = -1$ , and  $\det M_1^{(n)} = n - 4$ . With formula (8) this yields  $\text{tb}(L_0) = 0$  and  $\text{tb}(L_1) = 2 - n$ .

The Euler characteristic is  $\chi = n + 2$ , and from the Kirby moves in Figure 6 we read off  $\sigma = n - 1$ . The solution of  $M^{(n)}\mathbf{x} = \underline{\text{rot}} = (1, 0, \dots, 0)^t$  is

$$\mathbf{x} = (n - 1, -1, \dots, -1)^t,$$

hence  $c^2 = \langle \mathbf{x}, \underline{\text{rot}} \rangle = n - 1$ . With (3) this gives  $d_3 = \frac{1}{2}$ .

For the rotation number we observe that with

$$\underline{\mathbf{k}}_0 = (-1, \dots, -1)^t$$

and

$$\underline{\mathbf{k}}_1 = (-2, -1, \dots, -1)^t$$

we have

$$M^{-1}\underline{\mathbf{k}}_0 = (1, 0, \dots, 0)^t$$

and

$$M^{-1}\underline{\mathbf{k}}_1 = (2 - n, 1, \dots, 1)^t.$$

With (9) we obtain  $\text{rot}(L_0) = -1$  and  $\text{rot}(L_1) = n - 1$ .

REFERENCES

[1] M. S. BORMAN, YA. ELIASHBERG AND E. MURPHY, Existence and classification of overtwisted contact structures in all dimensions, *Acta Math.* **215** (2015), 281–361.  
 [2] F. DING AND H. GEIGES, A Legendrian surgery presentation of contact 3-manifolds, *Math. Proc. Cambridge Philos. Soc.* **136** (2004), 583–598.  
 [3] F. DING AND H. GEIGES, Legendrian knots and links classified by classical invariants, *Commun. Contemp. Math.* **9** (2007), 135–162.  
 [4] F. DING AND H. GEIGES, Legendrian helix and cable links, *Commun. Contemp. Math.* **12** (2010), 487–500.  
 [5] F. DING, H. GEIGES AND A. I. STIPSICZ, Surgery diagrams for contact 3-manifolds, *Turkish J. Math.* **28** (2004), 41–74.

- [6] F. DING, H. GEIGES AND A. I. STIPSICZ, Lutz twist and contact surgery, *Asian J. Math.* **9** (2005), 57–64.
- [7] F. DING, Y. LI AND Q. ZHANG, Tight contact structures on some bounded Seifert manifolds with minimal convex boundary, *Acta Math. Hungar.* **139** (2013), 64–84.
- [8] K. DYMARA, Legendrian knots in overtwisted contact structures, [arXiv:math/0410122v2](https://arxiv.org/abs/math/0410122v2).
- [9] YA. ELIASHBERG, Classification of overtwisted contact structures on 3-manifolds, *Invent. Math.* **98** (1989), 623–637.
- [10] YA. ELIASHBERG AND M. FRASER, Topologically trivial Legendrian knots, *J. Symplectic Geom.* **7** (2009), 77–127.
- [11] J. B. ETNYRE, Legendrian and transversal knots, *Handbook of Knot Theory*, Elsevier, Amsterdam (2005), 105–185.
- [12] J. B. ETNYRE, On knots in overtwisted contact structures, *Quantum Topol.* **4** (2013), 229–264.
- [13] J. B. ETNYRE, Convex surfaces in contact geometry, class notes, available at <http://people.math.gatech.edu/~etnyre/preprints/notes.html>
- [14] J. B. ETNYRE AND K. HONDA, Knots and contact geometry I. Torus knots and the figure eight knot, *J. Symplectic Geom.* **1** (2001), 63–120.
- [15] H. GEIGES, *An Introduction to Contact Topology*, Cambridge Stud. Adv. Math. **109** (Cambridge University Press, Cambridge, 2008).
- [16] H. GEIGES, A note on Legendrian knot complements, unpublished note, dated 11 January 2010; available upon request.
- [17] H. GEIGES AND S. ONARAN, Legendrian rational unknots in lens spaces, *J. Symplectic Geom.* **13** (2015), 17–50.
- [18] H. GEIGES AND S. ONARAN, Exceptional Legendrian torus knots, *Int. Math. Res. Not. IMRN*, to appear.
- [19] E. GIROUX, Une structure de contact, même tendue, et plus ou moins tordue, *Ann. Sci. École Norm. Sup. (4)* **27** (1994), 697–705.
- [20] E. GIROUX, Une infinité de structures de contact tendues sur une infinité de variétés, *Invent. Math.* **135** (1999), 789–802.
- [21] E. GIROUX, Structures de contact en dimension trois et bifurcations des feuilletages de surfaces, *Invent. Math.* **141** (2000), 615–689.
- [22] R. E. GOMPFF, Handlebody construction of Stein surfaces, *Ann. of Math. (2)* **148** (1998), 619–693.
- [23] R. E. GOMPFF AND A. I. STIPSICZ, *4-Manifolds and Kirby Calculus*, Grad. Stud. Math. **20**, American Mathematical Society, Providence, RI (1999).
- [24] K. HONDA, On the classification of tight contact structures I, *Geom. Topol.* **4** (2000), 309–368; erratum: *Geom. Topol.* **5** (2001), 925–938.
- [25] K. HONDA, On the classification of tight contact structures II, *J. Differential Geom.* **55** (2000), 83–143.
- [26] E. LERMAN, Contact cuts, *Israel J. Math.* **124** (2001), 77–92.
- [27] P. LISCA, P. OZSVÁTH, A. I. STIPSICZ AND Z. SZABÓ, Heegaard Floer invariants of Legendrian knots in contact three-manifolds, *J. Eur. Math. Soc. (JEMS)* **11** (2009), 1307–1363.
- [28] T. VOGEL, Non-loose unknots, overtwisted discs, and the contact mapping class group of  $S^3$ , *Geom. Funct. Anal.* **28** (2018), 228–288.

MATHEMATISCHES INSTITUT, UNIVERSITÄT ZU KÖLN, WEYERTAL 86–90, 50931 KÖLN, GERMANY

*E-mail address:* [geiges@math.uni-koeln.de](mailto:geiges@math.uni-koeln.de)

DEPARTMENT OF MATHEMATICS, HACETTEPE UNIVERSITY, 06800 BEYTEPE-ANKARA, TURKEY

*E-mail address:* [sonaran@hacettepe.edu.tr](mailto:sonaran@hacettepe.edu.tr)